2011

Development of a technique for achieving an optimum BSFC for LAF engine

Shreyash S. Ukidave
Michigan Technological University

Development of a technique for achieving an optimum BSFC for LAF engine

By
SHREYASH S UKIDAVE

A REPORT

Submitted in partial fulfillment of the requirements
for the degree of
MASTER OF SCIENCE IN MECHANICAL ENGINEERING

MICHIGAN TECHNOLOGICAL UNIVERSITY
2011

Abstract

The reserves of gasoline and diesel fuels are ever decreasing, which plays an important role in the technological development of automobiles. Numerous countries, especially the United States, wish to slowly decrease their fuel dependence on other countries by producing in house renewable fuels like biodiesels or ethanol. Therefore, the new automobile engines have to successfully run on a variety of fuels without significant changes to their designs. The current study focuses on assessing the potential of ethanol fuels to improve the performance of 'flex-fuel SI engines,' which literally means 'engines that are flexible in their fuel requirement.'

Another important area within spark ignition (SI) engine research is the implementation of new technologies like Variable Valve Timing (VVT) or Variable Compression Ratio (VCR) to improve engine performance. These technologies add more complexity to the original system by adding extra degrees of freedom. Therefore, the potential of these technologies has to be evaluated before they are installed in any SI engine. The current study focuses on evaluating the advantages and drawbacks of these technologies, primarily from an engine brake efficiency perspective. The results show a significant improvement in engine efficiency with the use of VVT and VCR together.

Spark ignition engines always operate at a lower compression ratio as compared to compression ignition (CI) engines primarily due to knock constraints. Therefore, even if the use of a higher compression ratio would result in a significant improvement in SI engine efficiency, the engine may still operate at a lower compression ratio due to knock limitations. Ethanol fuels extend the knock limit making the use of higher compression ratios possible. Hence, the current study focuses on using VVT, VCR, and ethanol-gasoline blends to improve overall engine performance. The results show that these technologies promise definite engine performance improvements provided both their positive and negative potentials have been evaluated prior to installation.

Acknowledgement

Although my name will appear on the front page of this report, the work done to complete this report would not have been possible without the guidance from my advisors, colleagues, family members and friends. It has been my honor to work in Michigan Technological University on a project funded by GM and State of Michigan through Michigan Energy Efficiency Grant (MIEEG case no. U13129). The challenging work and expectations from my research mates gave me an opportunity to work in a stressful environment and equipped me with a unique ability of finding my way through rock solid disasters. I would like to use this opportunity to thank the people who have helped me towards the completion of this report and gave me a chance to open myself for new adventures in life ahead of me.

First and foremost, I would like to thank my academic advisor Dr. Donna Michalek for her constant encouragement, detailed critique, timely follow ups and most importantly her understanding nature though out the course of my graduate studies at Michigan Tech. Her ability to push me when I was satisfied and quietly encourage me when I was in despair will always inspire me. Although her decision to leave Michigan Tech caused a great deal of distress at times, in the long run it provided me with wider breadth of experience. I must admit that her extraordinary compassion towards me and my work in her busiest schedule embarrassed me at times.

I am grateful to Dr. Jeff Naber for his immense technical guidance without which the goal of this report would have been impossible to achieve. He is one of the most generous people I have ever met in my life and his unwavering efforts to achieve his own goals will inspire me to achieve my own. His continuous support and wealth of knowledge in the area of internal combustion engines are the backbone of this report. I greatly appreciate his trust in me though out the completion of this report and would like to work with him in future if given a chance.

I would also like to acknowledge Jeremy Worm, Craig Marriot, Matt Wiles, Dustin Loveland and Dr. Abhijeet Mukherjee for interacting with me to share their experiences, give feedbacks and guide me on the right path even in their busy schedules. Their efforts though not seen directly have helped me to shape my ideas and achieve my goals.

I am extremely grateful to my colleagues Dr. Yeliana, Iltesham Syed, Vaibhav Kale, Abishek Manekar, Rajat Arora and Brandon Rouse for lovely working environment and friendly atmosphere they created and maintained. Their unconditional support and feedback on this report have to be acknowledged and appreciated without fail.

I would also like to thank my good friends Sabharwal, Virat, Gopi, Aniket, Animish, Aditya, Shantanu, Anand, Soumya, Gayatri, Akshay, Vikram, Parag and many others who have watched and helped me grow. It would have been a difficult task to complete this report without the crucial support from my friends. I also thank my parents for standing beside me and mentally supporting me whenever I was in distress. Without their financial and mental support I would have never imagined completing my graduation in a foreign university.

My special thanks go to Dr. Wayne Weaver for taking the time out of his busy schedule to review my report, showing willingness to attend my defense and be a member of my defense committee. With this I have thanked only a fraction of people and I would require another hundred pages to thank all of them. So grant me the permission to thank you all at once and I hope you enjoy reading each bit of this report.

Table of Contents

List of Figures

List of Tables

Nomenclature

EGR	Exhaust gas recirculation
BSFC	Brake specific fuel consumption
VVT	Variable valve timing
VCR	Variable compression ratio
VVA	Variable valve actuation
LHV	Latent heat of vaporization
MBT	Maximum brake torque
BMEP	Brake mean effective pressure
ECU	Engine control unit
SI	Spark ignition
CI	Compression ignition
I.C.	Internal combustion
HCCI	Homogeneous charge compression ignition
FMEP	Friction mean effective pressure
NMEP	Net mean effective pressure
MAP	Manifold absolute pressure
A/F	Air fuel ratio
CA50	50% burn location
ATC	After top center
RSM	Response surface modeling
ANN	Artificial neural network
CAD	Crank angle in degrees
IVO	Intake valve opening
IVC	Intake valve closing
EVO	Exhaust valve opening
EVC	Exhaust valve closing
LIVO	Late intake valve opening

LIVC	Late intake valve closing
LEVO	Late exhaust valve opening
LEVC	Late exhaust valve closing
RPM	Rotations per minute
PSO	Phasing schedule optimizer
LLC	Low lift cam
HLC	High lift cam
LPP	Location of peak pressure
COV	Coefficient of variation
WOT	Wide open throttle
PC	Personal computer
OS	Operating system
GM	General Motors
CA00	Combustion start angle
MW_{O2}	Molecular weight of Oxygen
MW_{N2}	Molecular weight of Nitrogen
MW_{H2}	Molecular weight of Hydrogen
MW_{C}	Molecular weight of Carbon
Φ	Equivalence ratio
γ	Specific heat ratio
η	Efficiency
x_b	Mass fraction burned
θ_0	Combustion start angle
$\Delta\theta$	Combustion duration
T_{ign}	Ignition temperature
P_{ign}	Ignition pressure
Sl_0	Laminar flame speed at reference condition
x_r	Residual gas fraction
ethv	Ethanol volume fraction

τ	Induction time
T	Induction time integral
KI	Knock intensity
A	Knock index multiplier
B	Activation energy multiplier
K_m	Percentage of unburned mass at knock initiation
V_{TDC}	Cylinder volume at TDC position
V_I	Cylinder volume at knock initiation
P	Pressure
ON	Octane number
thkn	Crank angle at knock initiation
T_a	Activation temperature (K)
T_u	Instantaneous unburned gas temperature (K)
B_p	Bowl bore
B_b	Piston bore
h_b	Bowl height
h_{cc}	Chamber height
V_c	Clearance volume
h_c	Clearance height

Chapter 1 Introduction

1.1. Background

Over the past decade researchers have developed new methodologies to assess and optimize engine powertrains. Conventional optimization techniques depend largely upon engine testing, due in part to the past computational limitations and lack of mathematical models that capture the stochastic nature of engine operation. The cycle-to-cycle and cylinder-to-cylinder variations in an engine limit the accuracy of predictions of engine performance at a variety of engine conditions. Test engineers can overcome this problem by exhaustive testing throughout the entire range of engine operation and by performing full factorial sweeps of independent variables that control engine performance. However there are several problems with this type of testing to optimize engine performance:

- Tests procedures are difficult to automate
- Different test conditions may demand different engine hardware setups resulting in increased testing time and effort
- Prototype engines are needed for testing
- Use of fuel and generation of pollutants

Though testing cannot be eliminated completely, the use of computers in engine optimization can greatly reduce the need for testing. Current advances in computational memory and speed have greatly enhanced the role of modeling and simulation in engine optimization.

A validation of the accuracy of mathematical models for predicting engine performance is necessary before using computer simulations in engine optimization. Predicting the stochastic nature of engine operation is difficult, but recent advances in computer technology allowing for more complexity, with some sacrifice of calculation speed, have

made it possible to build engine models that accurately predict the operation of actual engines.

In spite of these advances, the engine optimization process remains dependent upon a number of variables, and the correlation between different variables makes the task of optimization more difficult than ever. For example, the presence of cooled EGR is sometimes beneficial as it may reduce the knocking tendency of an engine operating in the high load region due to the charge cooling effect. Unfortunately, a high level of residual also increases engine variability while reducing fuel efficiency. Hence, engine calibration and optimization procedures often include finding trade-offs between different variables to obtain an optimum design.

This report includes a detailed description of an optimization technique developed for achieving an optimum BSFC target for LAF engine. The variables considered in the optimize process are VVT, VCR, spark timing, and fuel type. VVT, which is also referred to as VVA in the industry, can greatly increase fuel economy and also serve to minimize emissions. The full use of VVT requires variable valve timing and variable valve lift, but in the current report only variable valve timing is considered. The optimization strategy of VVT is highly dependent on the specific engine operating point under consideration and involves trade-offs between BSFC, variability, residual gas fraction, idle quality, and emissions.

VCR is a promising technology to increase the thermodynamic efficiency of engines, but at higher compression ratios knocking increases significantly possibly damaging engine parts and causing unstable operation. To counteract the problem of knocking at higher compression ratios, the octane requirement of the engine is increased. The easiest way to increase the octane rating of fuel is to add alcohol to conventional fuels. For example, the addition of ethanol to regular unleaded gasoline considerably enhances engine

performance at high load and speed operating conditions. Figure 1.1 shows the historical increase in ethanol use as a transportation fuel.

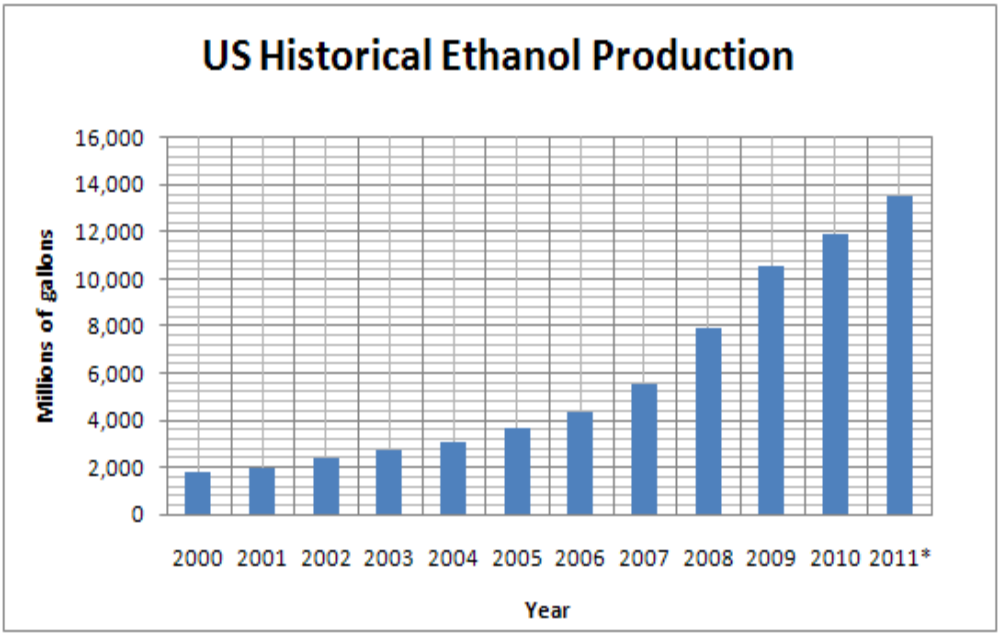

Figure 1.1: Historical Fuel Ethanol Use [1].

One major disadvantage of using ethanol blended fuels is the decreased power output per unit mass of fuel due to the lower LHV of ethanol. However the improvements achieved in knocking tendency and emissions make it worthwhile to use ethanol blends instead of regular unleaded gasoline. The addition of ethanol in gasoline increases the latent heat of vaporization, which in turn gives a charge cooling effect. The charge cooling effect plays an important role in reducing cylinder temperatures, which increase the density of air, thereby increasing the volumetric efficiency of the engine.

Spark timing is also of paramount importance to satisfactory engine operation. There is an optimal spark timing at which an engine produces maximum torque, referred to as

Note: (* value indicates the anticipated use in year 2011)

MBT timing. The MBT timing can change considerably as the operating conditions of the engine change. The general test procedures for selection of MBT timing consist of sweeping the spark manually and observing the BMEP in real time, but this procedure can be cumbersome. Hence a simpler but more accurate approach is required to find optimum spark timing. A possible solution may be to capture the trends and magnitudes of changes in MBT timing with speed and load conditions, use these values in the ECU in a table format, and select the optimum timing in real time. Modeling and simulation engineers can further simplify the MBT timing selection technique by including genetic algorithms and neural networks and using sophisticated industry standard programming tools like MATLAB and SIMULINK. If such tools are inaccessible, engineers can use a more direct and robust approach as recommended by Design of Experiments to determine MBT timings.

1.2 Motivation

1.2.1 Importance of Study

From an efficiency perspective, I.C. engines are not the best choice to generate power, but for mobile applications they dominate the market. Traditionally, I.C. engines are classified into two categories, namely SI and CI engines. CI engines with turbochargers, superchargers, and EGR systems can reach efficiencies as high as 45% because of the use of higher compression ratios. SI engines generally operate at lower compression ratios due to knock limits, and therefore they have lower fuel efficiency as compared to CI engines. Hence current research is focused on developing HCCI engines, which are fundamentally a combination of SI and CI engines. Researchers are also studying variable compression ratio engines, the use of bio-fuels to raise knock limits, VVT, plug-in hybrids, and lower displacement turbocharged SI engines. All of these strategies for increasing the SI engine efficiency are promising, but some of them are not yet fully understood. For example, VVT can increase the volumetric efficiency of engines, but the

fundamental and physical basis of this increase in volumetric efficiency is not yet understood in full detail.

The automotive market is and will continue to be competitive. With energy costs constantly rising, the State of Michigan and auto manufacturers are conducting research on flex fuel vehicles, hybridization, alternative fuels, and efficiency improvements. The commitment of GM to lead the development of new technologies for better engine performance is clear with over 3 million flex fuel vehicles sold since 2008 year [1]. GM has also introduced eight hybrid models with a promise of launching plug in hybrids during years 2010-2012, which will further reduce dependence on foreign oil. To reap the rewards of these different technologies used in conjunction with each other, system integration studies have to be performed. For example, to efficiently incorporate VVT with flex fuel technology, it is very important to understand how these two technologies influence each other to properly calibrate the engine. The current study, performed with a GM standard one dimensional model developed using GT-POWER, focuses on understanding the potential of new technologies like variable compression ratio, VVT, and flex fuels used in conjunction with each other.

1.2.2 Development of GM-Michigan Tech Predictive Combustion Model Tool

The current advances in computer software used for engine simulations have simplified the task of optimization. Moreover, simulation plays an important role in feasibility studies of new designs. Apart from saving money and time in engine testing, simulations also provide the advantage of automating the optimization process. The most widely used engine simulation tool, GT-POWER, has advanced tremendously in its capability to accurately predict actual operating engine performance. Also, the simplicity and user friendliness of this product have made it an industry standard tool to simulate engine processes.

The selection of software depends upon the problem to be solved. In the current project, GT-POWER was extensively used to optimize performance at given operating conditions. GT-POWER can also be interfaced with third party software programs like KIVA or SIMULINK, which make it easy to extend the simulation capabilities. The use of MATLAB also makes algorithm development easier. In recent years genetic algorithms have been developed to predict uncertainties in biological data. Engine researchers are successfully using these algorithms to predict the stochastic nature of engine operation [4-5]. In addition, data handling and analysis are simplified with the use of MATLAB mainly because of special toolboxes designed to perform specific tasks, e.g. the statistical toolbox.

GT-SUITE is a family of software programs containing the engine modeling tool GT-POWER [2]. Other tools in GT-SUITE can model valve trains, cooling and thermal management, drive trains, after-treatment, and fuel injection. The availability of these models built within the family set of GT-SUITE can facilitate the task of complete vehicle performance. Hence, the GT-POWER was used to model and simulate the engine performance in this project.

1.2.3 Model-based Engine Optimization

The current Mathworks model-based engine calibration toolbox makes engine calibration less cumbersome with minimal user interference to the process [4-5]. The basic idea behind this toolbox is to handle the complexity of multi-objective optimization, while satisfying the constraints. For example, in a gasoline engine case study with spark timing and compression ratio as input variables, BSFC as object variable, and knock as a constraint variable, this toolbox can directly determine the optimum BSFC point given the test/simulated data. The need for a specific algorithm to develop an optimization

strategy is completely eliminated in this process. This type of optimization tool has great potential because of the reduced complexity and time in calibrating engines. This type of direct optimization tool developed by Mathworks has been a constant motivation in the optimization algorithm development within the current study. A specific program was written in MATLAB that can interactively determine an optimum solution given inputs from the user such as operating points or constraint variables. The user has great flexibility in choosing numerical values for the constraint variables. Though the current program is not as robust as the model calibration toolbox, it is definitely an important and successful step toward achieving the target of optimization.

1.3 Goal and Objectives

1.3.1 Goal

The goal of the project is to develop an optimization technique for achieving an optimum BSFC target for LAF engine.

1.3.2 Objectives

The project goal was achieved through the following objectives:

- Update the GM-Michigan Tech predictive combustion modeling tool with improved correlations and models developed by the GM/Michigan Tech research team.
- Using a Design of Experiments methodology, simulate engine performance using sweeps of compression ratio, VVT, ethanol blend, and spark timing.
- Analyze the resulting simulation data and explain the observed trends.

- Fit parametric functions to BSFC, which correlates engine fuel efficiency to operating conditions such as VVT, compression ratio, ethanol fraction, and spark timing.

A GT-POWER predictive combustion compound model was developed at Michigan Technological University [6]. This combustion model captures in-cylinder combustion phenomenon based upon correlations of burn durations with non-dimensional engine parameters. With further studies in chemical kinetics, the existing correlations were changed to a newer and more accurate version for ethanol fuel blends [7]. A Chen Flynn friction submodel was also included to accurately capture the speed and maximum in-cylinder pressure effects on FMEP. In addition a simple knock submodel was included to observe the trends and magnitudes of knock and apply knock constraints while optimizing BSFC. The model was updated to account for differences in clearance heights due to chamber geometries. The current updated calculations determine the clearance height corresponding to the combustion chamber geometry under consideration.

The study utilized a Design of Experiments methodology to optimize BSFC at five given operating conditions by sweeping compression ratio, VVT, ethanol blends, and spark timings. The large number of variables involved in the study complicated the trend analysis. Hence, apart from BSFC, it was important to track additional variables such as the heat release rate. This study was of paramount importance in developing parametric functions of BSFC at different load and speed points.

1.4 Overview of the Report

The remainder of the report is divided into four subsections, namely the literature review, model development, results and discussions, and conclusions and recommendations. In the literature review, findings of the past research in the same field are discussed in

detail. Though the present report does not include engine testing, the literature review includes some discussion of test results. The model development chapter details the modifications made to the GT-POWER compound model to incorporate new mathematical correlations. This chapter explains the capabilities added to the existing base LAF engine model such as the Chen Flynn friction mechanism and knock predictions. The simulation matrix and operating points used for optimization are also included in this chapter. The results and discussions chapter explains the findings of the study. In some cases the results do not correlate with past studies and the author has tried to provide possible explanations for the anomalies. The conclusions and recommendations chapter details the advantages and disadvantages of the technologies studied in this report and their potential to improve engine performance.

Chapter 2 Literature Review

2.1 Introduction

Several engine parameters that affect the engine performance will be discussed in this chapter along with the techniques used to optimize engine fuel efficiency. The author will review the fundamentals as well as recent research in the field of engine optimization with emphasis on an explanation of the sensitivity of engine performance to independent control variables such as spark timing and air fuel ratio.

2.2 Fundamentals of Gasoline Engine Performance

The general performance of SI engines is normally assessed using two quantities. The maximum brake power indicates the peak output of the engine, while the maximum brake torque indicates the breathing capacity of the engine at all speeds. If an engine has satisfactory maximum brake power and torque, the next step is to fine tune the variables to optimize BSFC, while satisfying standards for emissions or knock. There are many variables that affect SI engine performance, but only the most important variables like speed, load, and valve timing will be discussed here.

2.2.1 Air-Fuel Ratio

The capability of any engine to extract energy from burnt fuel depends largely upon the air-fuel ratio of the inducted mixture. Every engine has optimum fuel conversion efficiency at a specific air-fuel ratio. The main reason for this is that the chemical reactions that govern the release of fuel energy as it is burnt change according to mixture composition. Before the fuel is completely burnt and all the products of combustion are

released, the fuel goes through thousands of chain reactions. The complete mechanism of these chain reactions is not yet fully known, but the current computational research into combustion phenomenon shows that for gasoline engines the maximum burning temperatures are attained at an air-to-fuel ratio equal to 14.7. This value of 14.7 is determined using combustion stoichiometry, as represented by the following reaction

$$C_a H_b + \left(a + \frac{b}{4}\right)(0_2 + 3.76N_2) = aCO_2 + \frac{b}{2}H_2O + 3.76\left(a + \frac{b}{4}\right) \quad [2.1]$$

where C_aH_b is the hydrocarbon under consideration. The air-fuel ratio for the complete burning of any hydrocarbon, denoted as C_aH_b, can be calculated as

$$\textbf{Air to fuel ratio} = \frac{\text{mass of air}}{\text{mass of fuel}} = \frac{\left(a + \frac{b}{4}\right)(MW_{O_2} + 3.76 \times MW_{N_2})}{(a \times MW_C + \frac{b}{2} \times MW_{H_2})} \quad [2.2]$$

In Equation 2.2 MW_C, MW_{H2}, MW_{O2}, and MW_{N2} are the molecular weights of carbon, hydrogen, oxygen, and nitrogen, respectively. Based upon Equations 2.1 and 2.2, the complete burning of gasoline (C_8H_{18}) requires an air-fuel ratio equal to 14.7. This air-fuel ratio is referred to as the stoichiometric air-fuel ratio. The general trend in the engine research community is to use the quantity Φ, which is given by

$$\phi = \frac{\text{stoichiometric air to fuel ratio}}{\text{actual air to fuel ratio}} \quad [2.3]$$

where ϕ in the above equation is called the equivalence ratio. Gasoline engines perform well at an equivalence ratio between 1.0 and 1.1.

The thermodynamic efficiency of an engine is proportional to the adiabatic flame temperature of combustion. Hence, the higher the adiabatic flame temperature, the better the performance. The adiabatic flame temperature changes with the air-fuel ratio. Theoretically, complete combustion of the fuel results in the highest adiabatic flame temperature. The dependence of adiabatic flame temperature on the air-fuel ratio is shown in Figure 2.1.

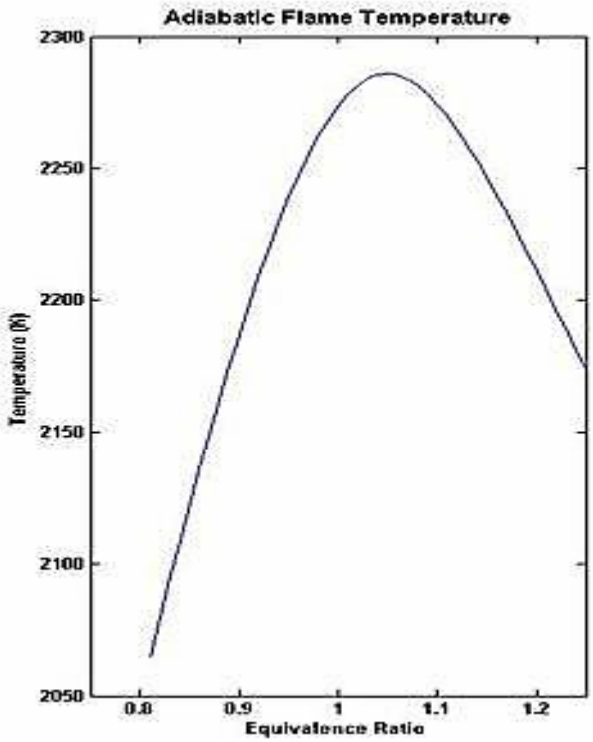

Figure 2.1: Variation of Adiabatic Flame Temperature with Equivalence Ratio.

Data used to generate the plots in Figure 2.1 were obtained using CANTERA, which is an open source software package that uses a reduced mechanism for gasoline fuel. As can be seen from Figure 2.1, gasoline yields a peak adiabatic flame temperature at an equivalence ratio of 1.05. Theoretically, gasoline should produce a peak adiabatic flame temperature at ϕ=1.0, but the actual equivalence ratio required to achieve the best fuel conversion efficiency is slightly greater than 1.0. The reason for this behavior of gasoline

fuel may be the dissociation of molecular oxygen at high in-cylinder temperatures. Therefore, while theory predicts that the fuel is completely burnt leaving no excess oxygen in the product species, this is not generally the case, as some oxygen is formed due to dissociation. Hence some excess fuel can be burnt, increasing the temperature due to the heat released from this combustion.

The optimum equivalence ratio for a given combustion chamber varies greatly with load and the speed point under consideration. For example, at very low loads it may be beneficial to use a fuel-rich mixture to increase the flame speed of the mixture composition. At part loads it may be beneficial to use a fuel-lean mixture for two reasons: 1) increases in the specific heat ratio value and the air dilution of the mixture increase the expansion work, and 2) as excess air is drawn in to dilute the mixture, it increases the intake pressure, decreasing the pumping loss. However, from an NOx emissions perspective, it is advantageous to use a stoichiometric mixture because a three-way catalyst in aftertreatment achieves the best possible reduction in NOx close to stoichiometry. Due to current stringent emission standards, SI engines generally operate at a stoichiometric air-to-fuel ratio. Hence, in this report, the equivalence ratio is not considered as a control variable, and engine simulation results are obtained at ϕ=1.0.

2.2.2 Spark Timing

Spark timing has a considerable effect on brake torque. Generally at a given engine speed the engine produces maximum torque. This optimum timing is called maximum brake torque timing (MBT). Figure 2.2 shows that for a given spark timing the engine produces maximum torque for a constant speed and air fuel ratio. The general guidelines used for correlating maximum brake torque timing with mass burning profile and maximum cylinder pressure are: 1) for MBT timing, maximum cylinder pressure occurs at 16° ATC [8], and 2) for MBT timing, the CA50 location is at 10° ATC [8].

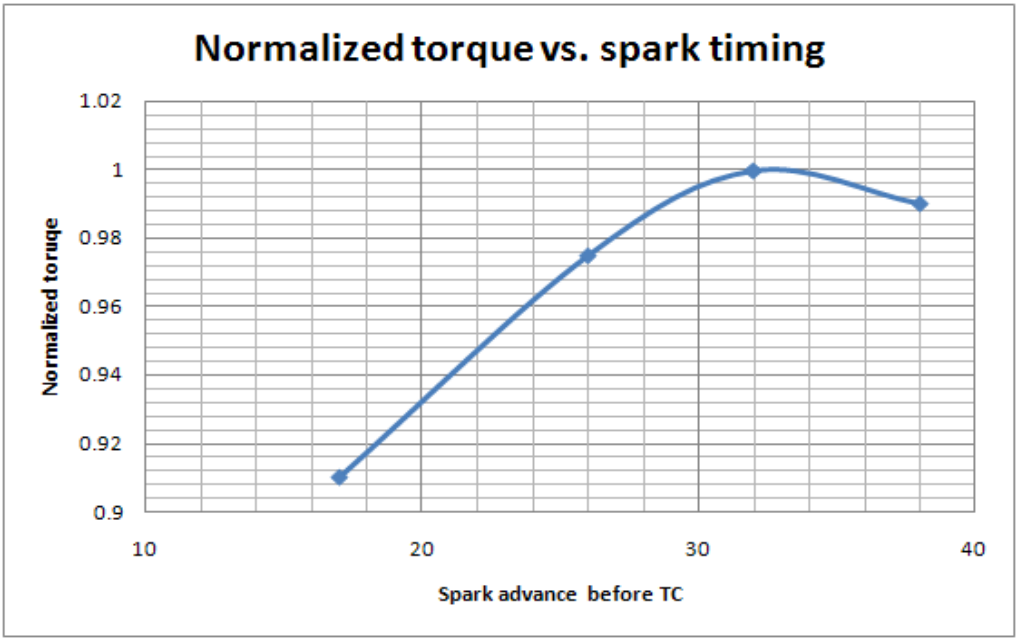

Figure 2.2: Effect of Spark Advance on Brake Torque at Constant Speed and Equivalence Ratio (data from [8]).

With the use of these empirical rules, we can change spark advance indirectly by changing CA50 locations to study the effect of spark advance on engine performance. In the GT-POWER simulations, this procedure of changing the CA50 location is generally employed due to the unavailability of a spark advance parameter as a control variable.

Apart from brake torque, spark advance also has a considerable effect on knock and emissions, particularly NOx emissions. Retarding the spark timing from the optimum may be useful for NOx emissions control as well as knock reduction, but at the same time it has to be remembered that retarding the spark too much reduces the output of the engine due to a greater loss of expansion work. Hence, engineers have to consider many factors before selecting optimum spark timing, and generally it is a trade-off between engine output, emissions, and knock.

2.2.3 Compression Ratio

Compression ratio has a direct effect on the indicated fuel conversion efficiency of the engine as shown by Equation 2.4

$$\eta_{\text{indicated}} = 1 - \left[\frac{1}{CR^{\gamma-1}}\right] \qquad [2.4]$$

where CR is the compression ratio and γ is the specific heat ratio of the mixture composition. Figure 2.3 shows the trend of indicated efficiency versus compression ratio for a γ=1.3.

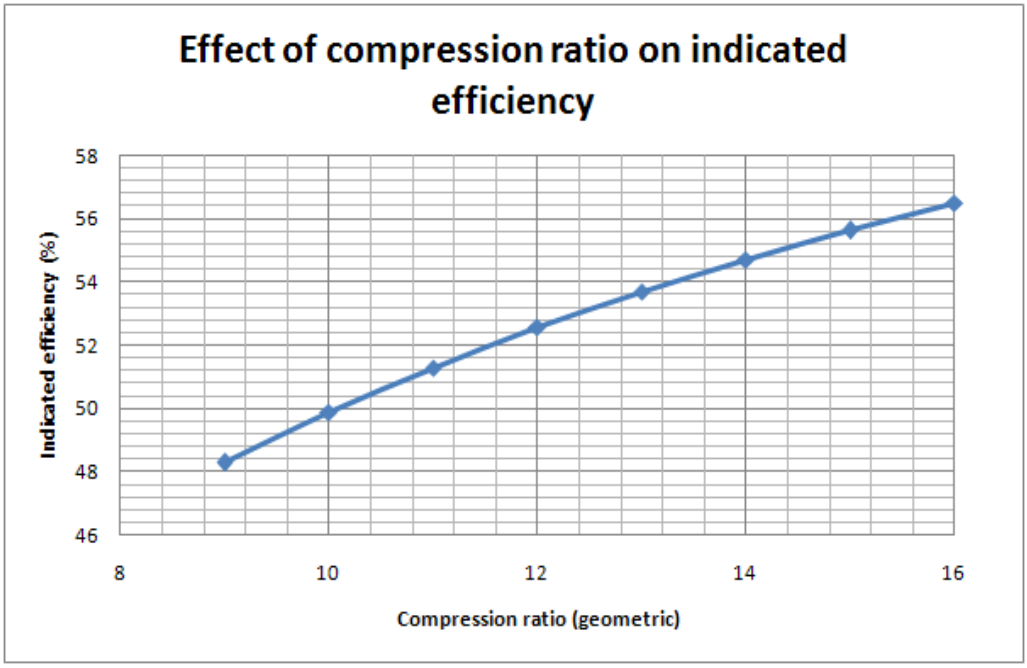

Figure 2.3: Variation of Indicated Efficiency with Compression Ratio.

Although it is desirable to increase the geometric compression ratio to increase indicated efficiency of the engine, the actual response of the engine to an increase in geometric

compression ratio is quite different. Compression ratio has an effect on heat loss, friction, and combustion phenomenon including combustion rates and stability. Hence, it is possible that if the geometric ratio is increased, the brake efficiency may not increase because the losses offset the gains obtained by the increase in compression ratio. Moreover, geometric compression and expansion are not achieved in actual engines due to valve timing effects, thus new terms such as effective compression ratio and effective expansion ratio are used to account for valve timing effects on cylinder mixture compression and expansion.

2.2.4 Load and Speed

The dependence of engine BSFC on load and speed is generally depicted through an engine contour map. To obtain a full BSFC map, exhaustive testing must be conducted over the full load and speed range of engine operation. The general aspects to consider while studying any engine map are:

- The mechanical efficiency decreases with an increase in speed due to increased friction. At the same time, due to the less time available at higher engine speeds, the heat transfer decreases [8].
- Starting at the lowest BSFC point, if we increase the speed at a constant load, BSFC increases primarily due to an increase in friction [8].
- Starting at the lowest BSFC point, if we increase the load at a constant speed, BSFC increases primarily due to mixture enrichment required to maintain the torque needed as engine breathing is greatly affected at low engine speeds [8].
- Starting at the lowest BSFC point, if we decrease the engine speed at a constant load, BSFC decreases primarily due to the increasing importance of heat transfer per cycle [8].

A generic engine map is shown in Figure 3.4.

2.3 New Developments and Technologies

2.3.1 Optimization Strategies

Current engine optimization techniques used during the engine design phase include interactive real time simulations that are interfaced with the hardware to automate the process. This process generally involves prior knowledge of the relationships between engine variables or use of adaptive algorithms. Rask and Sellnau [9] reviewed the process of automated engine calibrations in which they made use of GT-POWER 1D cycle simulations as a software in the loop system.

Rask and Sellnau presented a weighted operating point optimization technique that is now widely used in industry. With current industrial competition and the time available for powertrain development shrinking, more advanced methods of engine calibration are necessary. One way to approach this problem is to include high fidelity simulation software like GT-POWER in the loop. Use of VVA in powertrains adds additional degrees of freedom to the system increasing the required time for calibration, and hence sophisticated tools are necessary for engine calibration. VVA systems differ across the industry; some VVA technologies involve only timing control while others are more complex in nature, adding lift control as well. For example, optimizing 10 speed and load points at 10 intake and exhaust valve timings requires the results for and analysis of 1,000 cases. The addition of more degrees of freedom like EGR and variable valve lift substantially increases the complexity. Given the limitations of time and cost in dynamometer testing, the feasibility of conventional calibration techniques reduces exponentially.

Historically, people have approached the engine calibration problem in different ways. The Design of Experiments approach can be used efficiently to reduce dynamometer testing. In some cases, the RSM approach can be used to fit the object variable to the engine variables and predict the performance at non-tested points. The neural networks available in MATLAB can be used to automatically adapt to the trends. Such a tool is generally referred to as an ANN [10].

The basic requirements for use of simulation-based calibration are:

- Availability of output results at given operating conditions with full factorial sweep of control variables; or
- Partial test data availability with knowledge of trends, in which case Design of Experiments methods can be used to accelerate the calibration procedures; or
- Interfacing high fidelity engine simulation tools with adaptive control tools like neural networks, in which case the number of simulations can greatly decrease due to forward predictions of the trend.

All of these methods have been used by engineers, and they differ most significantly in the time associated with the calibration. While using a simulation environment for optimization, it has to be remembered that the ranges of the specified variables should be feasible. For instance, intake valve timing can be changed by 100 CAD, but it may not be possible from a design perspective to build such a flexible cam phaser.

It has been seen that as the engine model complexity increases by adding different submodels to predict NOx emissions, knock, and turbulent flame speed, the time required for the simulation to converge increases substantially. For example, when the GT-POWER model controller is used to control the torque by throttling the engine, it requires more time to converge with the addition of new submodels into the base model. One way to approach this problem is to use data tables and interpolation techniques instead of a controller. For example, a response surface can be fitted to the throttle diameter for a

given IVO and RPM combination. The simulation can refer to these tables and select the throttle diameter value in one step, instead of following a time consuming iterative convergence procedure. There may be some loss in accuracy of the control variable value, but it can be reduced by use of more accurate interpolation procedures.

Limitation of Simulation Methodology: Most of the simulation tools are equipped with steady state simulation platforms and either do not have transient simulation capabilities or do a poor job in predicting transient engine response. The allowable complexity of the model restricts its accuracy and, in some cases, the degrees of freedom of a given set of variables.

Constrained Optimization: Most of the time, it is required to quantitatively restrict some output quantities from a performance perspective. For example, most of the optimization problems have NOx emission constraints or knock limits. Rask and Sellnau [9] used a PSO to restrict the output quantities of interest to some desired value. In the PSO platform, the user has flexibility to input a value for a restrained quantity. For instance, the user can choose to limit the knock at high speed and load points, while neglecting the knock limits at idle conditions. Other quantities that can be restrained by the user are EGR limits and exhaust temperatures.

Study of the Two-Stage, Fully Capable VVA System: The study performed by Rask and Sellnau [9] involved deployment of two cam profiles, LLC and HLC. Their general algorithm involved simultaneous optimization of valve timing and lift profile. The procedure could vary, but the general guidelines that were applied to such a problem are optimizing the selection procedure of cam lift. For example, in the current study two cams can be used namely high lift and low lift cam, but to optimize BSFC the use of a low lift cam was found to be advantageous at engine loads below 600 kPa NMEP. Therefore 600 kPa was a threshold load that decided which of the two cams should be used. After selecting the cam, the valve timings were optimized for that particular cam.

The use of low lift cams at low loads considerably reduced the throttling losses due to increasing MAP.

Engines have a low volumetric efficiency at low loads because of the throttling of flow past the high lift cams, but with low lift cams engines were shown to have higher volumetric efficiency at low loads. This change in volumetric efficiency was achieved due to improvements in engine MAP with the use of low lift cams. It was also shown that pumping loss can be effectively reduced with the use of low lift cams. The main reason for the reduction in pumping loss was MAP improvement, which reduces air induction work. MAP had a direct effect on volumetric efficiency that in turn affected the pumping loss.

This strategy can contribute to building a "virtual dyno" for calibration, but calibration and optimization have to be extended further to calibrate the engine in less time. This is an achievable task due to computer advances, distributed computing, and the growing popularity of Design of Experiments techniques.

2.3.2 Variable Valve Timing

Variable valve timing is the next promising engine technology, which can take engines to new levels of performance in terms of efficiency, emissions, and maximum power. However, before VVT is actually put into practice it has to be tested, and its effects on engine variables have to be investigated. The complexity of VVT engines is considerably high compared to fixed cam engines, but the performance improvement achieved through this technology make it worthwhile to add more complexity in an engine by replacing fixed cam phasers with variable ones. Parvate Patil et al. [11] investigated VVT effects on an engine using a simulation environment and investigated the effects of VVT on

pumping loss, volumetric efficiency, BSFC, knock, and emissions. The authors used GT-POWER 1D cycle simulations for their analysis.

Late Intake Valve Closing (LIVC): Parvate-Patil et al. [11] concluded that LIVC reduces pumping losses. In a conventional engine the intake valve closes approximately 50 degrees after BDC, but if the intake valve is kept open for a longer duration some of the fresh air charge gets expelled back into the intake manifold during the compression stroke. This increases the manifold pressure, reducing the pressure gradient between atmospheric pressure and manifold pressure, which reduces the pumping losses of subsequent cycles. Moreover, there was an improvement in knock and emissions with the deployment of LIVC technology. LIVC reduced the effective compression ratio of the engine as some of the mixture returns to the intake manifold without being compressed. Hence, the cylinder pressures and temperatures at the end of the compression stroke are lower as compared to conventional engines, which results in lower combustion temperatures and pressures.

Late Intake Valve Opening (LIVO): Parvate-Patil et al. [11] found that late intake valve opening actually reduced unburned HC emissions. The reason is that LIVO created low pressure in the cylinder, which, when the intake valve was opened, created turbulence resulting in good combustion. However, the authors in this case failed to provide any data regarding combustion profiles or rates to substantiate their claims. It was also stated that while LIVO increases pumping losses, it does not affect volumetric efficiency significantly, but no striking evidence regarding this claim was given. LIVO methodology creates a vacuum condition in the chamber, and hence when the intake valve is opened the air rushes into the cylinder due to a pressure differential between the intake manifold and the chamber. Therefore it was assumed that LIVO would not have a detrimental effect on volumetric efficiency even though it increases the pumping losses. In the absence of any data/results regarding the combustion profile studied, it is risky to conclude that LIVO improved the combustion quality. One can claim that LIVO actually

reduced residual gas fraction due to less overlap between exhaust and intake, which may have a considerable role in improving combustion quality of the engine, but this also may be a premature claim in the absence of any combustion studies.

Early Intake Valve Closing (EIVC): Parvate-Patil et al. [11] concluded that early intake valve closing may prove beneficial at part loads as the mass of air required to burn low quantities of fuel is less because of the low torque requirements. In this method the intake valve is closed much earlier and the cylinder is isolated from the intake. This reduces the pumping losses as the piston does not have to do any work in the remaining intake stroke after the intake valve is closed. This improved the fuel economy but at the price of higher HC emissions, because less air results in poor combustion quality. This technology has more disadvantages than advantages and is still under investigation.

Early Intake Valve Opening (EIVO): Parvate-Patil et al. [11] also found that early intake valve opening means greater overlap between exhaust and intake, which results in higher residuals. The pressure gradient caused by these residuals enables flow back into the intake manifold from the cylinder. The residual gases, if contained in the cylinder are heated but as they flow back into the intake manifold, they are cooled due to heat transfer with the lower temperature fresh air mixture. In the subsequent intake stroke the residuals flow back into the cylinder at a lower temperature, reducing the overall combustion temperature, which results in decreasing knock and NOx emissions. However, EIVO has a downside because higher residuals reduce the mixture quality, reducing combustion quality and hence increasing HC and CO emissions.

When all or some of these technologies are used in conjunction with each other in an engine, it is possible that the gains obtained by one method are offset by another. Hence, it is difficult to optimize VVT to attain a target like BSFC while constraining undesirable parameters like knock and emissions to acceptable limits. Many times it has been observed that one particular set of timings gives better fuel economy and worse

volumetric efficiency, and engineers have to perform trial and error experiments to determine the optimum because of the highly stochastic nature of engines and lack of knowledge of the magnitude and direction of change in the engine variables involved.

Bozza and Torella [12] reviewed the use of 1D cycle simulations for A/F control in VVT engines. An experimentally calibrated map for different VVT positions is generally used for A/F control, but the disadvantage of such a method is the increase in complexity of ECU software to switch between volumetric maps as the VVT position changes. An alternative method to overcome this problem is to measure air flow with a flow meter in real time and feed the signal to an ECU so that the ECU can control the fuel injection parameters to ensure the required A/F ratio. However, this method adds complexity in hardware. Moreover, the flow meter readings may not be trustworthy in the presence of high residuals at high EGR rates. For these reasons the authors tried to develop correlations to calculate volumetric efficiency based upon engine variables like MAP, engine speed, and VVT position. The authors used a 1D IME code to simulate engine operation and validated the results at discrete load and speed points. This code was implemented to calculate of volumetric efficiency at different VVT positions.

Bozza and Torella [12] mainly observed LIVC and LEVC VVT technologies in conjunction with each other to study their effect on BSFC, knock, and emissions. These aforementioned VVT techniques when used in conjunction with each other resulted in a significant increase in fuel efficiency, while decreasing knock and NOx emissions. They reported a decrease in the burning speed of the mixture at high EGR rates, which decreased the combustion quality. The high EGR rates were a byproduct of LIVC and LEVC timings. To offset the downfall of poor combustion quality at these valve timings, they implemented a port deactivation strategy to induce swirl in the combustion chamber.

For part loads they defined the optimal VVT position by observing the trade-off between the reduction of pumping work and EGR rates, but the engine behaved very differently at

low loads. At low loads, retarding the cams increased COV of IMEP considerably. The 1D IME code used for numerical calculations was validated with the experimental results, but the authors failed to validate the code at a variety of load and speed points. As discussed in this study performed by Bozza and Torella [12], the parameters in the code, used similarly to flow coefficients in pipes or back pressures in the exhaust, were tuned only for WOT performance. Hence, this code is not a good representation of engine behavior at part and low loads. Nevertheless, the BSFC and volumetric efficiency trends observed at part loads provided good insight into the behavior of engine variables when subject to VVT technologies.

After validating the numerical 1D IME code at a variety of engine load conditions, it was used to calculate engine variables at 64 operating points with a full factorial sweep of VVT. The point to be considered here is that a full factorial sweep is not generally required and is undesirable to perform because of the computational time and cost constraints. The authors could have used Design of Experiments procedures, now widely used in industry, to reduce the number of simulations. The time required to perform the full factorial sweep on a single PC AMD Athlon 1.7 GHz with Linux OS was two weeks. Based upon simulation results, they attempted to fit a correlation to volumetric efficiency as shown below,

$$\eta_{vol} = a_1\left\{\frac{RPM}{1000}\right\}^2 + a_2\{VVT\}^2 + a_3\{MAP\}^2 + a_4\left\{\frac{RPM}{1000}\right\}\{VVT\} + a_5\left\{\frac{RPM}{1000}\right\}\{MAP\} + a_6\{MAP\}\{VVT\} + a_7\left\{\frac{RPM}{1000}\right\} + a_8\{VVT\} + a_9\{MAP\} + a_{10} \quad [2.5]$$

where are $a_1..a_{10}$ are regression coefficients. This type of second order polynomial fit the data very well; however, it is complex due in part to the presence of nine correlation parameters. Some of the regression coefficients are quantitatively small enough so that

the parameter they are associated with can be neglected. For instance, the coefficient a_2 in the above correlation is -0.00005878 and, hence, the term $[VVT]^2$ can be easily dropped, reducing the complexity of the equation.

Bozza and Torella [12] also ran the simulations with a variety of ambient pressures and temperatures to observe the dependence of volumetric efficiency on reference conditions. They observed a linear dependence of volumetric efficiency on the temperature-over-pressure ratio due in part to the sound speed variations and heat loss effects. The presented study greatly simplified the A/F ratio control in a VVT engine to resemble a fixed cam engine with the only addition being a cam position sensor. By sensing the cam position, the volumetric efficiency of the engine can be predicted using the correlations, significantly reducing the complexity of A/F ratio control strategy.

2.3.3 Variable Compression Ratio Engines

Diesel engines are more efficient than gasoline engines, and this has given diesel engine manufacturers an advantage in today's competitive market. Over the past several years most of the diesel engine manufacturers have implemented turbochargers and superchargers for boosting purposes, but boosting technologies in the case of gasoline engines are still not popular. Schwaderlapp et al. [13] reviewed the potential of boosting technology in conjunction with variable compression for gasoline engines. The variable compression ratio, if applied to gasoline engines along with a boosting device, can be as efficient as diesel engines.

The selection of compression ratio for a gasoline engine is based mainly on the knock limit at high load. Hence, most often engines have to be designed for a lower compression ratio than they can withstand at part load. The knocking tendency of an engine at part load is considerably less because of lower combustion temperatures and

pressures. Hence, they can tolerate higher compression ratios at these loads, but if the engine has a fixed compression ratio, then their part load efficiency is affected. As most engines operate at part load conditions for most of their life-time, this results in a considerable loss of fuel efficiency.

A solution to this problem is moderately simple and may be summarized as downsizing engine displacement along with implementation of boosting and variable compression ratio capabilities. The downsizing of the engine moves the operating point of the engine to a lower BSFC zone by increasing the specific load on the engine and decreasing friction and pumping work. Downsizing reduces the fuel consumption and friction, while increasing the losses associated with the increase in compression ratio and reduced displacement.

Schwaderlapp et al. [13] have shown through experimental data that downsizing of the engine displacement by 40% can achieve an increase in overall efficiency by 12.3%. However, during the process of downsizing any engine, the compression ratio has to be reduced due to knocking. As the engine becomes incapable of running at the same compression ratio, its thermodynamic efficiency reduces. To overcome this loss, variable compression has to be attained with modifications in the configuration of the engine. There are several methods of achieving variable compression, but the discussion of these methods is beyond the scope of this report.

Nilsson et al. [14] formulated an optimal control strategy for fuel control in SI variable compression ratio engines. In conventional engines knock is avoided by retarding the spark timing from the optimum. Though knock is avoided by late combustion, this also decreases engine efficiency. Variable compression ratio engines give one more degree of freedom to help avoid knock by adding a capability to reduce the compression ratio, but the presence of two control variables obviously poses a vital question of selection of the values to obtain the best engine efficiency.

Nilsson et al. [14] studied the dependency of engine efficiency and IMEP on compression ratio and ignition timing at a variety of load and speed conditions. The objective variable of the optimization was fuel consumption, while the constraint applied was knock intensity. The torque models were fitted to the experimental data, and the authors successfully showed that a higher compression ratio resulted in greater engine torque and therefore greater efficiency. The knock was measured by applying a high pass filter and setting a window length of 25 samples. The authors considered only the knock intensity at the primary knock frequency of 7 to 8 kHz, but this introduced some errors in the calculation of knock intensity as knock also occurs at secondary frequencies much higher than the primary one and, if not considered, can cause engineers to inaccurately quantify the knock [15].

Nilsson et al. [14] showed that at low loads the knock intensity was less sensitive to ignition angles. The increase in spark advance at low loads increased knock intensity smoothly over the range of ignition angles. Moreover, at low loads the advantages of a higher compression ratio can be fully realized because of lower knock tendency. The knock trends change considerably at part and higher loads. The 100 kPa MAP is close to full load for a naturally aspirated engine, but the engine under experimental investigation here was equipped with a turbocharger and, hence, able to run at MAP pressure above atmospheric. At 100 kPa MAP, the sensitivity of knock to ignition angle and compression ratio increased significantly. The behavior of the engine knock at this load with respect to ignition angle was quite abrupt. Moreover at this load it was impossible to run the engine at a compression ratio of 14 because of high knock intensities even at retarded ignition timings.

2.3.4 Gasoline-Ethanol Blending

Recent government legislation will require mandatory use of 10% ethanol in gasoline-fueled engines in the future. These ethanol-blended gasoline fuels are generally referred as "gasohol." High content ethanol such as 85% is currently available in select locations in North America. The main motivations for use of renewable fuels are the depleting petroleum resources, lower emissions, and better engine performance. With the renewable nature of ethanol fuels, a possibility exists in the near future to convert current vehicles into flex-fuel vehicles that can run on a wide range of ethanol-gasoline blends without any change in engine design. This requires the performance of current engines to be optimized for various ethanol blends. Ethanol fuels also have some limitations, which pose challenges in designing an optimized engine capable of running on flex-fuel. The basic difference between ethanol and gasoline fuel is shown in Table 2.1.

Table 2.1: Fuel Properties (data from [16])

	Gasoline	Ethanol
Lower heating value (MJ/kg)	42.7	26.8
Density (kg/m^3)	715-765	790
Octane number(R+M/2)	86-90	100
Latent heat of vaporization (kJ/kg)	380-500	904
Stoichiometric air-fuel ratio	14.7	9
Self-ignition temperature (°C)	~300	420
Laminar flame speed (m/s)	~3.3	~3.9

As shown in Figure 2.4, the addition of ethanol decreases the energy content of the mixture per unit mass, but the advantages of using ethanol-blended gasoline fuels include better performance, reduced emissions, and increased efficiency. Ethanol has a considerably higher octane number rating than gasoline, reducing the knock tendency and making possible the use of a higher compression ratio at higher loads. Moreover, the higher latent heat of vaporization of ethanol serves to improve the performance of the

engine. However, it has some negative effects on engine operation especially at cold starting conditions.

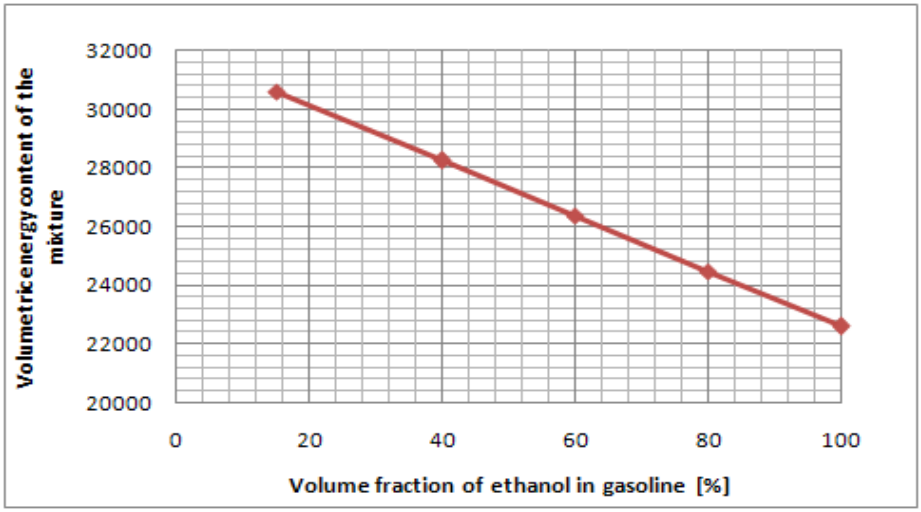

Figure 2.4: Energy Content [kJ/liter] as a Function of Blend Ratio (data from [16]).

Wallner and Miers [16] have investigated the combustion characteristics of gasoline-ethanol blends in SI engines. They studied the variation of brake thermal efficiency with the addition of ethanol and observed that at low and medium loads pure gasoline and low ethanol blends gave approximately the same brake thermal efficiency. They also observed that at higher loads the efficiencies for higher ethanol blends increased continuously, whereas those for lower ethanol blends and gasoline deteriorated. This is due to the fact that if the engine is equipped with a knock sensor, at higher loads and for low ethanol blends and gasoline, it retards the spark timing from optimum to avoid the knock. The retarded spark timing decreases the engine efficiency, but the spark timing at higher ethanol blends, like E85, can be kept at the optimum without any potential hazard of knock. This is shown in Figure 2.5. The optimum spark timings for limited knock for each fuel are shown in Figure 2.5 along with their corresponding 50% mass fraction burn locations in Figure 2.6.

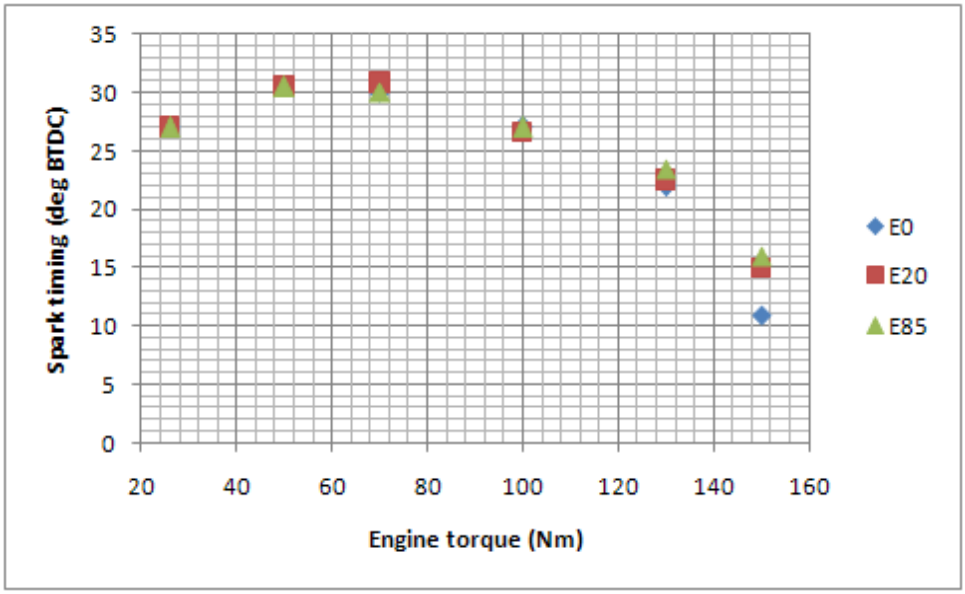

Figure 2.5: Optimum Spark Timing versus. Engine Torque (data from [16]).

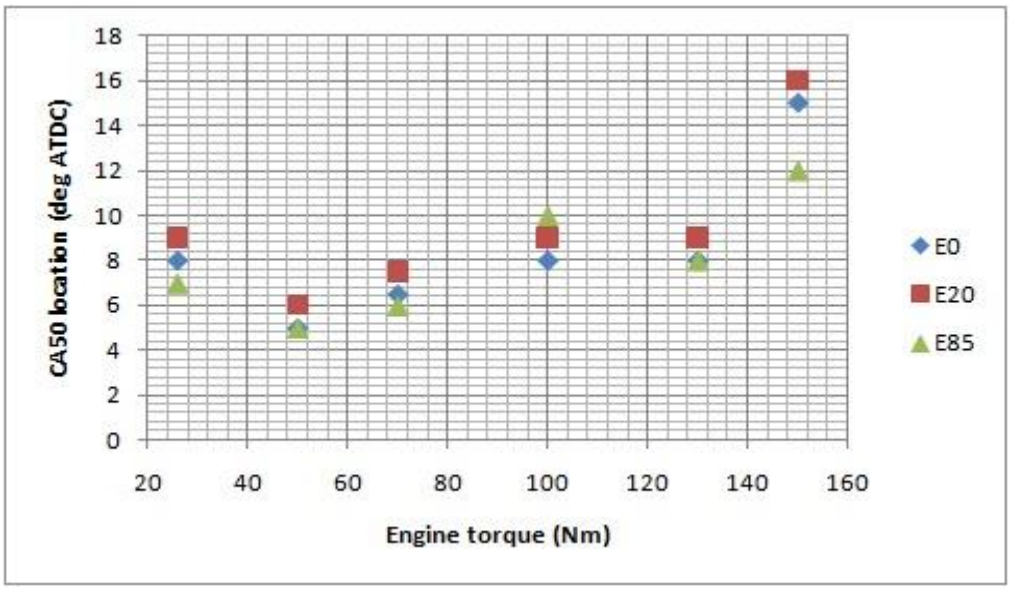

Figure 2.6: CA50 Location versus. Engine Torque(data from [16]).

Evident from Figure 2.5 is the effect of fuel on combustion phasing. At low and part loads the spark timing for each fuel was approximately at the optimum with some minimal differences, but at high loads the spark timing for gasoline and low ethanol blends has to be retarded to avoid knock. This results in a later CA50 location thereby decreasing the efficiency, but for E85, even at high loads, spark timing near the optimum can be realized, keeping the knock index within permissible limits. It should be noted that the feasibility of combustion phasing can also be determined from the location of peak pressure instead of the 50% mass fraction burn location.

Figure 2.7 shows the effect of peak pressure location on the indicated mean effective pressure for different ethanol blends. It should be stated that the indicated mean effective pressure is directly correlated to engine torque. From Figure 2.7 it is clearly seen that for E85 the peak pressure location can be advanced considerably compared to gasoline and low ethanol blends.

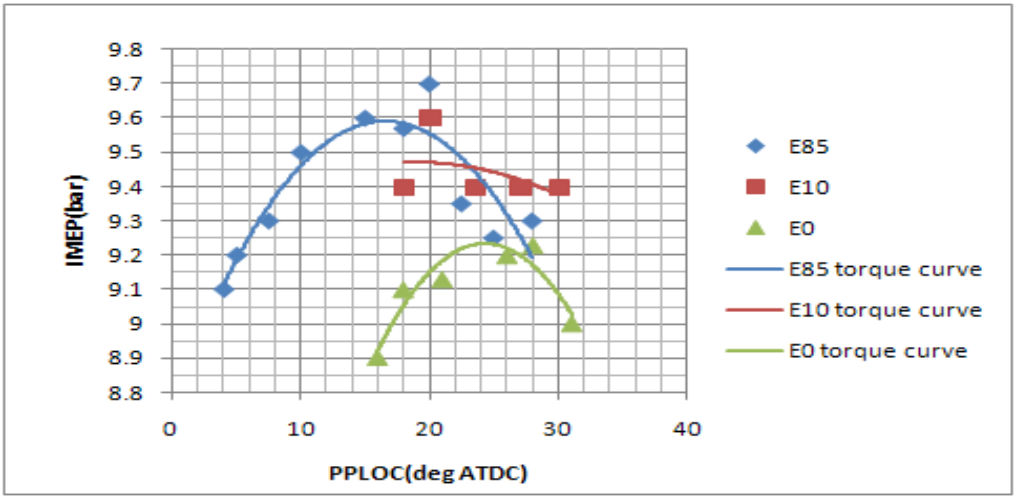

Figure 2.7: IMEP Comparison for Different Fuels (data from [17]).

It can be argued that differences in the IMEP of each fuel, as seen in Figure 2.7, are caused primarily by the air-to-fuel ratio and heating value variations in these fuels. If one

considered the lower AFR for E85 along with its lower heating value, then the E85 mixture yields the same energy content per unit mass of mixture charge as gasoline and, hence, the source of differences in IMEP is other than AFR and heating value. Wallner and Miers [16] did not provide volumetric efficiency differences for these fuels, which could explain the differences in IMEP values. From a fundamental perspective, higher latent heat of vaporization should cool the incoming air increasing its density and, hence, volumetric efficiency of the engine. It is known that the engine needs a greater amount of ethanol blended fuel as compared to pure gasoline to output the same torque. This extra fuel displaces some air after vaporization and decreases the volumetric efficiency. Thus the overall volumetric efficiency is the same or slightly less for E85 than for gasoline.

Figures 2.8 to 2.10 show the effect of ethanol addition on emissions. It is clear from these figures that ethanol addition significantly decreases the CO and HC emissions from the engine. This is due to the effect of oxygen enrichment on ethanol blends. Each ethanol molecule brings with it one atom of oxygen, which results in lean combustion because of the increased stoichiometric air-to-fuel ratio.

At the same time ethanol addition has a detrimental effect on NOx emissions. The NOx emissions for ethanol blends are higher than gasoline because of higher combustion temperatures. As explained earlier, with ethanol blends optimum spark timing can be achieved, resulting in greater combustion temperatures, but with gasoline the spark timing has to be retarded from the optimum, which has an adverse effect on engine efficiency but reduces NOx emissions because of sub-optimal combustion pressures and temperatures.

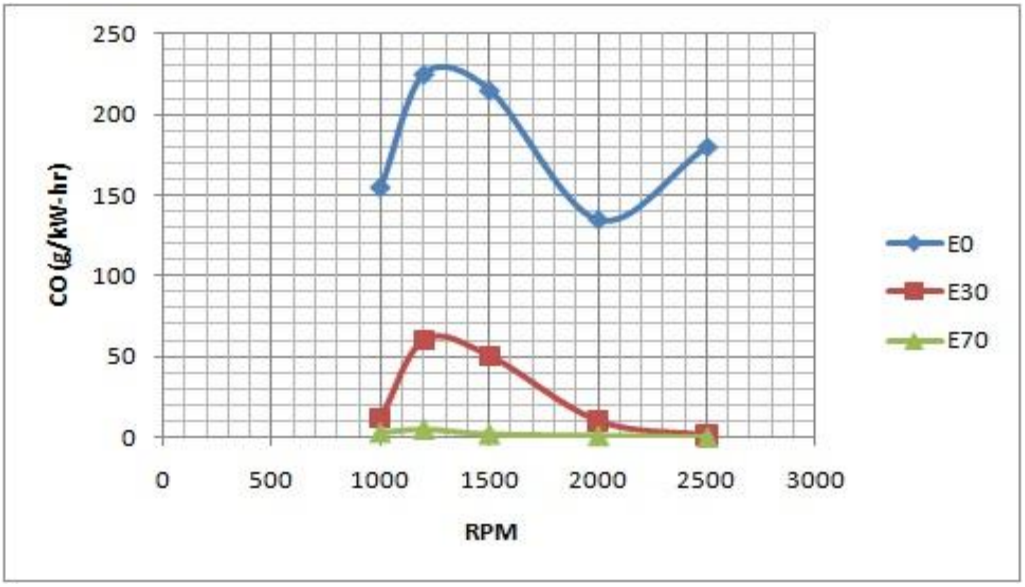

Figure 2.8: CO Emissions for Different Fuels (data from [17]).

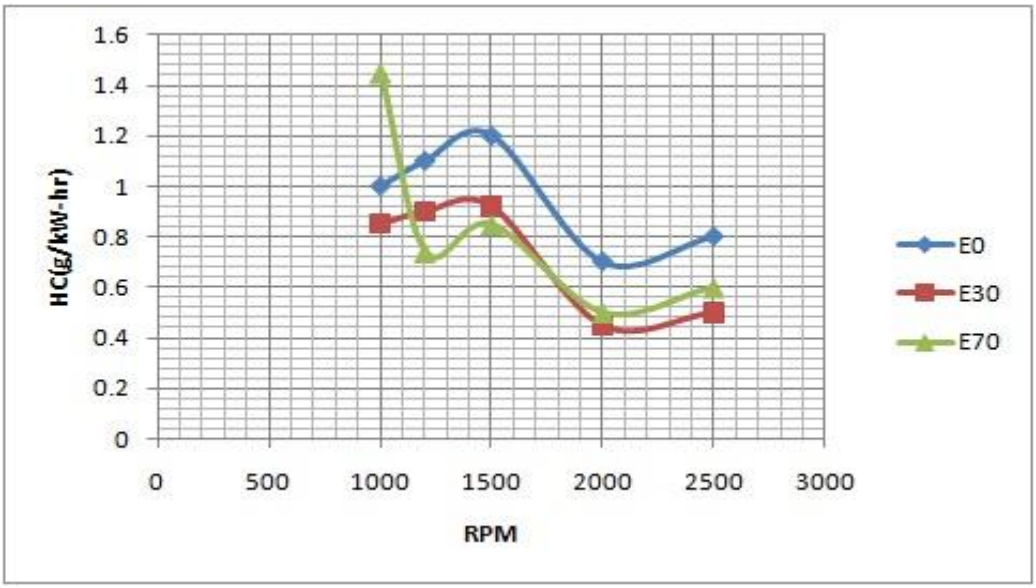

Figure 2.9: HC emissions for different fuels (data from [17]).

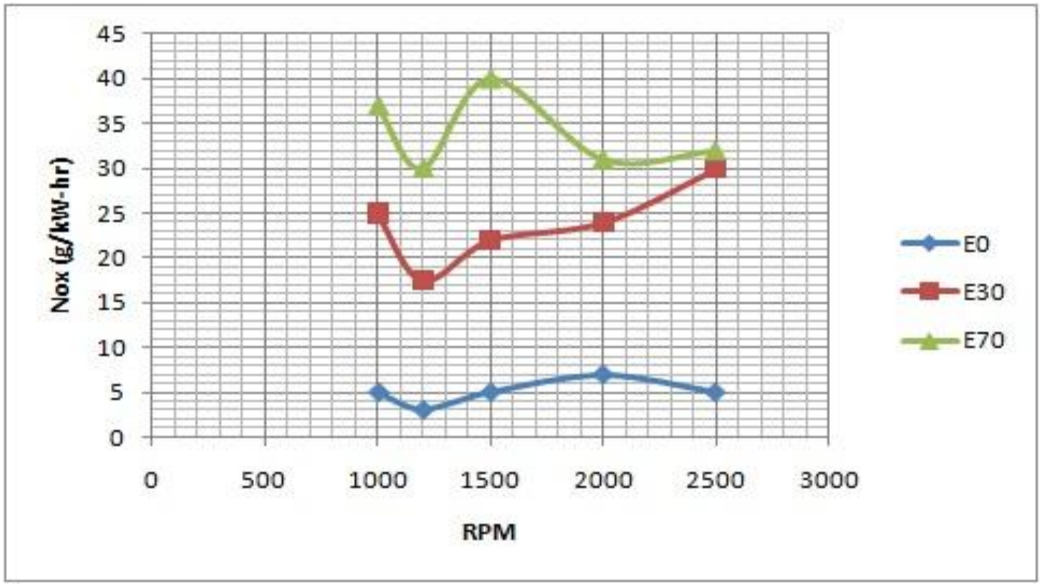

Figure 2.10: NOx Emissions for Different Fuels (data from [17]).

Chapter 3 Model Construction

3.1 Background

To assess the performance of any engine it is important to study the in-cylinder combustion in explicit detail as the combustion characteristics have the greatest affect on the overall engine performance. The intake and exhaust pressures primarily affect the volumetric efficiency of the engine, while combustion affects the fuel conversion efficiency. There has been a significant amount of research performed on the topic of in-cylinder combustion, but assessing the uncertainty in combustion due to cycle-to-cycle variation is very difficult. Recently a predictive combustion modeling tool was developed at Michigan Tech through a research project funded by GM and the State of Michigan. This tool makes use of parametric correlations to predict the mass fraction burned based upon known input conditions such as engine geometry, chemical properties of the fuel, and operating conditions. The detailed description of the model can be found in Yeliana [6]. Herein only the changes made to the existing tool will be discussed.

The predictive combustion model was built using the GT-SUITE [5] software platform. GT-POWER is a subset of GT-SUITE in which in-cylinder combustion, turbulence, flame characteristics, fuel spray entrapment, and knock can be modeled. GT-POWER contains in built-in single Wiebe function model that is widely used to calculate the mass fraction burned profiles. The general form of the single Wiebe function is

$$x_b = 1 - \exp[-a\left(\frac{\theta - \theta_0}{\Delta\theta}\right)^{m+1}] \quad [3.1]$$

where x_b is the mass fraction burned, a and m are shape factors, which can be varied, θ_0 is the reference angle, and $\Delta\theta$ is the combustion duration. GT-POWER takes θ_0 as the CA50 location and $\Delta\theta$ as the burn duration 10-90% [5]. Accordingly, the values of the parameters a and m change, but Heywood states that θ_0 is the start of combustion and $\Delta\theta$ is the total burn duration ($x_b = 0$ to $x_b = 1$). Figure 3.1 shows a comparison between an MFB profile calculated using single Wiebe model and an experimentally obtained MFB. As can be seen, the single Wiebe accurately represents the mass fraction burned profile in this case, and hence has a potential for use in engine combustion studies. However, by analyzing Eqn. 3.1, it can be determined that it provides a poor fit to asymmetrical mass fraction burned profiles.

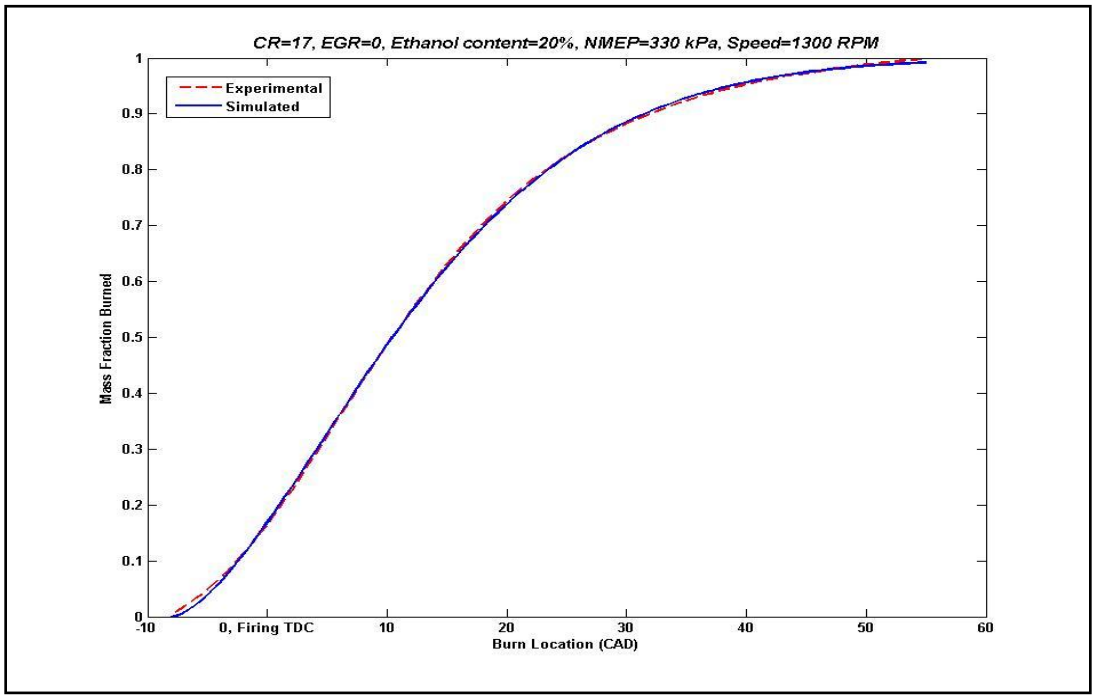

Figure 3.1: Comparison of Experimentally Obtained and Wiebe Model Generated Mass Fraction Burn Profiles.

In some circumstances a single Wiebe function cannot predict the MFB with sufficient accuracy, especially when the burn profile is not a smooth exponential function. For

example, when engine burning rates are rapid in the first half of combustion and decrease in the later half, it has been observed that a single Wiebe does a poor job of representing the mass fraction burned profile. In such cases a double Wiebe has proven to be more accurate. The GT-POWER compound model used for this study incorporates a double Wiebe model to approximate the combustion profile, which is first calculated using several burn duration correlations [6].

3.2 Model Updates

In this chapter a brief explanation of the changes made to the existing GT-POWER combustion compound model is presented. It will discuss the following topics:

- Laminar flame speed calculations
- Chen Flynn mechanism for calculating engine friction
- Knock model
- Clearance height calculations for different combustion chamber geometries
- Simulation matrix and operating points

3.2.1 Laminar Flame Speed Calculations

The GT-POWER combustion compound model uses a set of burn duration correlations that include laminar flame speed. The laminar flame speed calculations are performed explicitly in the model, and then the calculated laminar flame speed is used as an input to the burn duration correlations. The existing laminar flame speed correlations use a constant coefficient of 2.3 for residual gas fraction, which was shown to change with changes in fuel type [7]. Hence the form of the correlation was changed to accurately predict the laminar flame speed for each fuel type. Using research conducted at

Michigan Tech in the field of chemical kinetics, more robust and accurate correlations for the laminar flame speed were developed [7]. The existing laminar flame speed correlations available in GT-POWER are

$$Sl = Sl_0 \times \left(\frac{T_{ign}}{300}\right)^{\alpha} \times \left(\frac{P_{ign}}{1.01325}\right)^{\beta} \times (1 - 2.3 \times x_r) \quad [3.2$$

$$Sl_0 = (1 + 0.7 \times ethv^{0.35}) \times (0.4658 \times \phi^{-0.326}) e^{(-4.48 \times (\phi - 1.075)^2)} \quad [3.3$$

$$\alpha = 1.56 + 0.23 \times ethv^{0.46} \quad [3.4]$$

$$\begin{aligned} &\phi > 1: \beta = 0.22 \times (1 - ethv) - (0.17 \times ethv \times \sqrt{\phi}) \\ &\phi <= 1: \beta = 0.22 \times (1 - ethv) - (0.17 \times \frac{ethv}{\sqrt{\phi}}) \end{aligned} \quad [3.5]$$

This was changed to the modified laminar flame speed correlation of

$$Sl = Sl_0 \times \left(\frac{T_{ign}}{300}\right)^{\alpha} \times \left(\frac{P_{ign}}{1.01325}\right)^{\beta} \times (1 - a \times x_r)^b \quad [3.6$$

$$Sl_0 = (1 + 0.7 \times ethv^{0.35}) \times (0.4658 \times \phi^{-0.326}) e^{(-4.48 \times (\phi - 1.075)^2)} \quad [3.7]$$

$$\boxed{\begin{array}{l} ethv <= 0.69 : \alpha = 1.86, \beta = -0.42, a = 1.4, b = 2.3 \\ ethv > 0.69 : \alpha = 1.95, \beta = -0.40, a = 1.55, b = 1.97 \end{array}} \quad [3.8]$$

Equations 3.6 to 3.8 are used to calculate the laminar flame speed at the start of combustion, CA00. To calculate the laminar flame speed at 50% burn angle, T_{ign} and P_{ign} in the above correlations are replaced by T_{CA50} and P_{CA50}. Temperatures and pressures at the start of combustion and at the 50% burn angle are calculated in the GT-POWER model during the previous iteration and sent to the laminar flame speed submodel. The submodel calculates the laminar flame speed as an input to the burn duration correlation. Using the burn duration correlations, the model calculates the burn profiles, pressures, and temperatures. The entire loop is repeated until the convergence criteria are met. The GT-POWER compound model can be found in Appendices A and B.

3.2.2 Chen Flynn Mechanism for Calculating Engine Friction

Engineers use heat release models to predict the engine performance with reasonable accuracy making possible the prediction of cylinder pressure history. Using the heat release and volume change rate of the combustion chamber, indicated quantities like mean effective pressure, power, and torque can be predicted. However, prediction of brake output quantities can be difficult and incorrect at times because of the inadequate models that are used to calculate the mechanical losses. Significant portions of these losses are attributed to various types of frictional losses namely piston assembly friction, valve train friction, bearing friction, and losses in auxiliaries. Hence it is important to calculate the friction accurately to make reliable predictions of brake quantities.

The studies performed by R. E. Gish et al. [18] showed the dependence of engine friction on engine speed and peak cylinder pressure. These studies are the origin of the Chen Flynn friction model, which accounts for the dependence of engine friction on engine speed as well as combustion pressure. Over the years the Chen Flynn model has been

used by countless engineers to predict friction losses with reasonable accuracy. However, there are disadvantages of this formulation e.g. regression of model coefficients for a new dataset or engine configuration. This model lacks true predictability in terms of its ability to calculate frictional losses for a completely unknown engine configuration. Nevertheless, this model can be used satisfactorily whenever reliable experimental results are available.

The problem of inaccurate predictions of engine friction with the Chen Flynn model lies mainly in accounting for the friction from different engine components that respond differently to changes in pressure, temperature, load, and speed. S. F. Rezeka et al. [19] proposed a model to calculate engine friction on a crank angle basis instead of cycle basis. This type of formulation proved to be very accurate and has been improved by other engineers over the past years. As discussed earlier, engine friction is divided into many categories and some of these categories show little to no dependence on engine speed and load. For example, the valve train friction is independent of engine speed and load, and is a strong function of crank angle. Therefore, assuming that valve train friction is dependent on speed and load reduces the accuracy of friction prediction. This is the case with other friction components like piston skirt friction, unloaded bearing friction, and ring viscous friction, which show more dependence on crank angle than on speed and load.

Another factor that reduces the accuracy of the Chen Flynn model is its dependence on an engine dataset that is used to calculate indicated quantities [20]. If the test set up or design parameters are changed, then the model coefficients have to be recalculated to maintain the accuracy. This is a hindrance to obtaining fast results in competitive environments. Moreover, it has been shown that model coefficients developed for one geometrical configuration of an engine cannot be used for a different geometry due to a lack of reliability [20]. Another conclusion drawn by E. Pipitone [21] showed that friction is not only dependent on the magnitude of peak cylinder pressure but also on its

crank angle resolved location. They showed considerable improvement in accuracy of friction prediction by adding LPP as a fifth term in the Chen Flynn model.

The Chen Flynn friction model tries to capture the dependence of engine friction on engine speed and predict FMEP using a mathematical formulation with the general form

$$\boxed{FMEP = A + B \times P_{\max} + C \times n + D \times n^2} \qquad [3.9]$$

where *A*, *B*, *C*, and *D* are constants. It has been shown in the literature [22] that the Chen Flynn model predicts the FMEP within an error of 10%. Some recent work has examined the inclusion of a fifth term in the above formulation to represent the location of peak pressure [21]. This type of formulation has been shown to be more accurate than the Chen Flynn model, but for the current project, the Chen Flynn model was used to calculate FMEP with four terms as shown in Eqn. 3.9.

Engine friction is also dependent on engine geometry parameters such as bore, stroke, piston weight, and piston skirt. Hence the general practice is to determine new values for *A*, *B*, *C*, and *D* for each engine geometry. The dependence of engine friction on speed and load was also studied at Michigan Tech, and it was observed that two engines operating at the same speed and load can show vast differences in FMEP values as calculated by the Chen Flynn model. The following figure shows this difference.

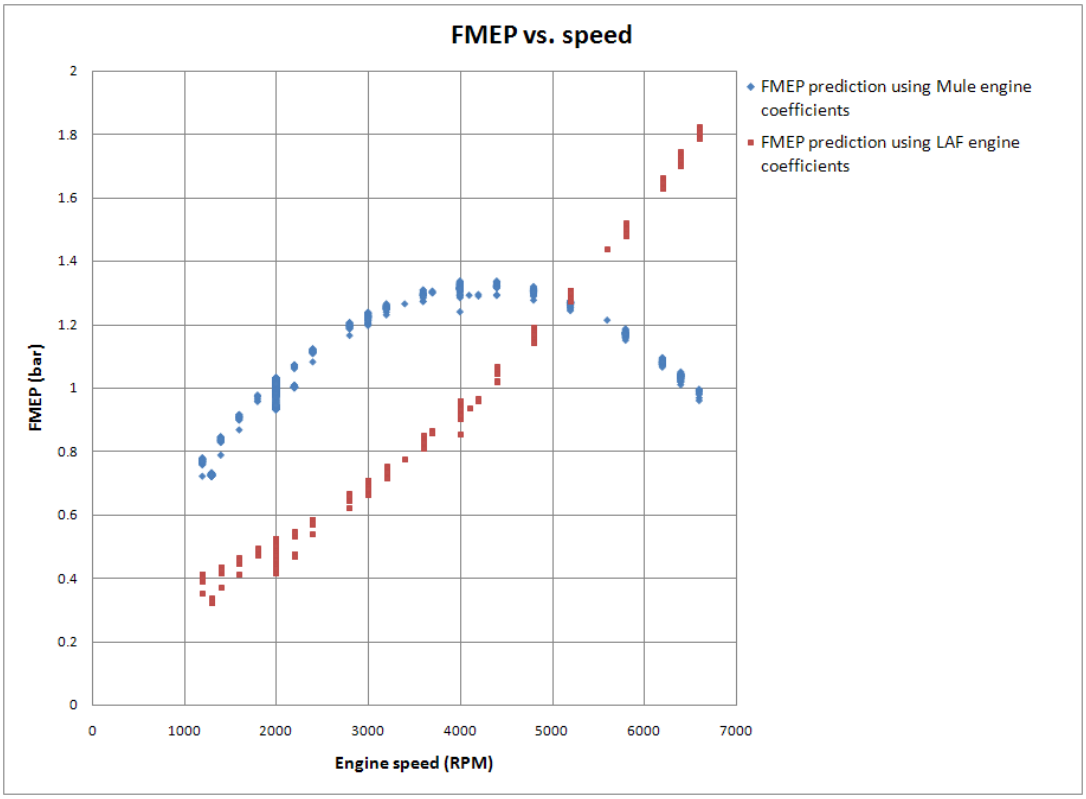

Chen Flynn FMEP= constant+(mean piston speed factor*mean piston speed)+ (mean piston speed factor^{2}*mean piston speed$^{2)}$+(peak pressure factor*peak pressure)

	Mule coefficients	LAF coefficients
Mean piston speed factor	0.156	0.0166
Mean piston speed factor^{2}	-0.0056	0.0025
Peak pressure factor	0.0015	0.0016
Constant	0.125	0.1736

Figure 3.2: Comparison of Chen Flynn Model FMEP Calculations for LAF Engine using LAF and Mule Coefficients.

As can be seen from Figure 3.2, using Mule engine coefficients to predict FMEP for the LAF engine leads to inaccurate results. The FMEP should physically rise with an increase in engine speed, but for the speed of 4000 RPM and above the FMEP values obtained using the Mule coefficients start to drop, even with increasing speed. This

problem can be overcome by obtaining new model coefficients based on the LAF dataset. The LAF coefficients describe the engine friction accurately. However, the accuracy of the Chen Flynn model can further be improved by the use of methods described previously.

3.2.3 Knock Model

For most cases knock provides a constraint to the engine optimization problem. In the current project, a knock model was used in GT-POWER to predict knock intensity, which was used to remove high intensity knock cases during the optimization process. The implemented knock model calculates knock intensity based upon the Douaud and Eyzat formulation [5] for in-cylinder knock. This formulation is widely used to calculate knock intensity as the calculations are less complex than those of other available formulations such as Franzke and Worret [5]. The inputs to the knock model are combustion chamber geometry, spark location, and octane number.

The current project includes knock intensity as a constraint variable rather than an object variable, and therefore the required accuracy of the value for knock intensity is less severe. Hence, for the current study, a simple engine with a flat chamber and bowl in piston geometry was specified. The spark plug was located centrally in the chamber and 2 mm from the dome head.

The octane numbers for the fuel blends (E10, E20, and E85) were taken from the CARB report [23]. There has been significant disagreement among the octane numbers results for ethanol blends obtained by different test engineers. The octane number of gasoline fuel does not increase linearly with the addition of ethanol, and hence engineers have performed experiments to calculate the octane number of a given gasoline-ethanol blend instead of predicting it based upon a formulated function. Because of this variation in octane numbers, it was necessary to use a single source for the octane number of the fuel

blends being considered. The CRC report does contain octane ratings for E10, E20, and E85, and hence this report was used to obtain representative octane ratings.

As can be seen from Figure 3.3, the octane rating of an ethanol blend is not proportional to the percentage of ethanol in the blend. The greatest increase in octane number occurs between E0 and E10, but then remains essentially constant to a level of 85% ethanol in the blend. The difference between the (R+M)/2 value of E0 and E10 is 4%, while between E10 and E85 it is 7%. The octane number value specified in the GT-POWER knock model is the (R+M)/2 value.

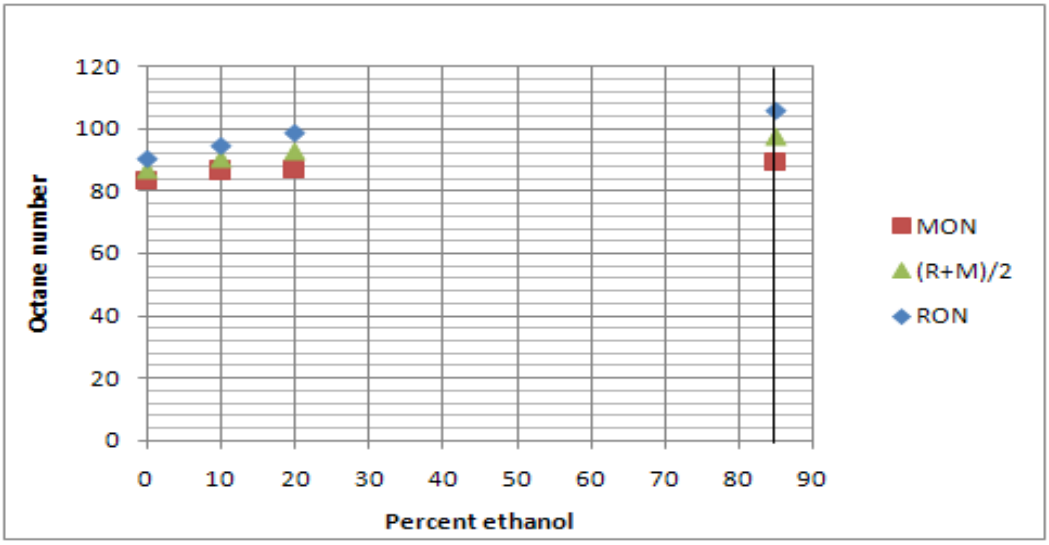

Figure 3.3: Effect of Ethanol Addition on Octane Number.

The knock model determines a global value of knock intensity, which is based on the induction time integral calculated for all of the individual surfaces in contact with the unburned gas. The model divides the space between the unburned gas and individual surfaces into thin zones of gas. The temperatures of these thin zones are calculated based on the bulk gas temperature and adjacent wall temperature and further used to calculate the induction time integral [5].

The Douaud and Eyzat [5] formulation of knock intensity is divided into two subparts, which are represented by Equations 3.10 through 3.12. Equations 3.10 and 3.11 calculate the induction time and its integral, respectively, and Equation 3.12 calculates the global knock intensity based upon the methodology describes previously. The induction time integral is evaluated from intake valve closing angle to the angle at knock initiation. When the value of this integral is greater than one, the cycle is considered to be knocking. Equation 3.12 calculates the global knock index value for the cycle under consideration.

$$\tau = 5.27 \times 10^{6} \times P \times \left(\frac{ON}{100}\right)^{3.402} \times P^{-1.7} \times e^{\left(\frac{3800}{B \times T_u}\right)} \qquad [3.10]$$

$$T = \int_{IVC}^{thkn} \frac{1}{\tau}.dt \qquad [3.11]$$

$$KI = 10^{4} \times A \times K_m \times \left(\frac{V_{TDC}}{V_I}\right) \times e^{\left(\frac{-T_a}{T_u}\right)} \times \max[0,(1-(1-\phi)^{2})] \times T_{avg} \qquad [3.12]$$

The knock intensity value calculated by the GT-POWER knock submodel is a global value and is a representation of the severity of knock. To correlate this value with the actual knock intensity for a specific engine, there are several multipliers that increase or decrease the severity of the knock. Due to the limited availability of knock behavior knowledge for the LAF engine, the multipliers were set to default values of 1. The next step was to correlate the GT-POWER knock intensity values with experimental data representative of the LAF engine knock behavior. Data from the Michigan Tech Hydra engine, a single cylinder version of the 4 cylinder LAF engine, was used for this purpose. The GT-POWER model for the Hydra engine was used to correlate the calculated knock

model intensity results with actual engine knock intensity values at given operating conditions.

A rigorous model calibration would include extensive experimental testing and scaling of the GT-POWER knock model coefficients to produce results that match the experimental knock intensities. Such a calibration technique is complex due to the number of parameters that affect engine knock. For example, spark advance can considerably increase the knock probability and intensity, but at the same time IMOP and EMOP can also affect it. In general, to capture the sensitivity of knock to different engine parameters, all the parameters are swept in their respective ranges and then these results are used to calculate the knock model coefficients, but due to a lack of data from such a test a less comprehensive approach was used to calibrate the knock model.

The Hydra engine test data collected by Brandon Rouse consists of averaged values of each measured quantity for 150 cycles at each test point [24]. Due to the inherent cycle-to-cycle variability, ACAP recorded spark timings and CA50 locations for each cycle. Though the actual sweep of spark timing was not taken during testing of the Hydra engine, the presence of cyclic variations in spark timing can be used effectively. Hence to calibrate the knock model, the GT-POWER Hydra model was run at three IMOP and EMOP conditions with a sweep of CA50 location from 0 to15 CAD ATC. The results from the sweep of CA50 locations for each IMOP and EMOP condition were exported to MATLAB [25] for analysis. These data are shown in Appendices C, D, and E.

It is clear from Figure 3.4 that the knock intensity does not vary linearly with CA50 advance, but exhibits a sudden increase after a particular value of CA50. To calibrate the knock model, it is necessary to define a border line knock intensity beyond which the engine is considered to be knocking. This border line knock intensity value can be found by comparing the simulation results of knock intensity to the experimental data. The

experimental border line knock intensity value for the Hydra engine was defined as 30kPa by Brandon Rouse [24].

From the experimental data, three test conditions were chosen at which the engine was running in the border line knock condition. The same cases were run in GT-POWER by performing a sweep of CA50 in the Hydra model. The simulation results were compared to test results and the knock model was calibrated. The border line knock intensity value for the GT-POWER knock model was assumed to be 600 units and any case with a knock intensity value higher than 600 was considered to be in the knocking region. The results of the comparison between experimental knock intensities and simulated knock model intensities are shown in Appendices C, D, and E.

3.1.5 Simulation Matrix and Operating Points

In this study, the operating points selected for the optimization were based on the engine map of a 2010 Chevy Malibu provided by GM. The engine map and 11 operating points are shown in Figure 3.6. Determination of the number of points used for optimization is based on similar studies conducted by GM which used three, five, and 11 points for optimization depending upon the required accuracy of the results and resources devoted to the project. From the 11 points provided, five points were used for the current optimization. These operating points were calculated for FTP cycle considering equal regions of work at all of these points. Hence the results can be obtained faster for five operating points than for 11 with minimal loss of accuracy. Table 3.1 shows the five operating points used for optimization in the current study. The corresponding values of torque, speed, power, and fuel consumption are also shown in Table 3.1. Table 3.2 shows the range of each GT-POWER input variable, namely IMOP, EMOP, compression ratio, CA50 location, and fuel type.

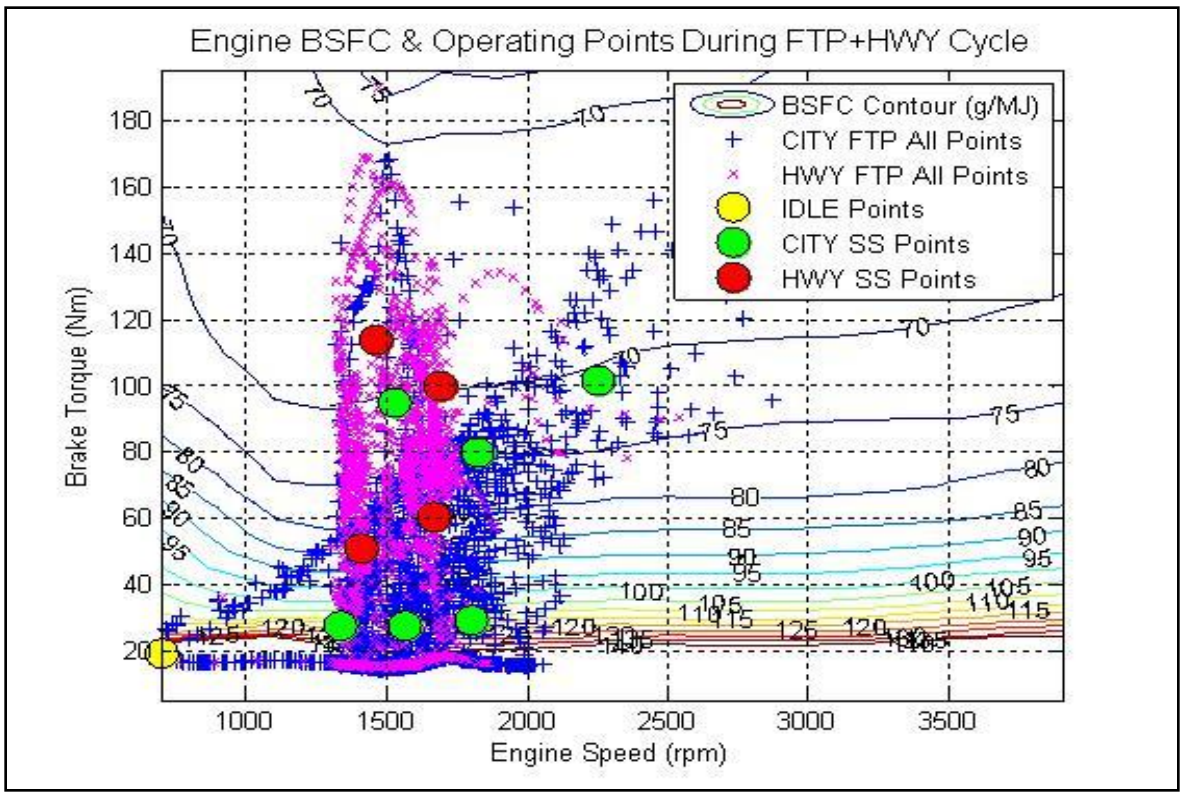

Figure 3.4: Engine Map of Chevy Malibu 2010 with 11 Operating Points.

Table 3.1: Specifications for Operating Points

Time weighted operating points within regions of equal work (5 points)				
	Engine Speed	Engine Torque	Fraction of Engine Work	BSFC
	RPM	Nm	Percent	g/MJ
Idle	700	19.05	4.75	136.2
Zone 1	1541	28.05	47.44	112.64
Zone 2	1814	90.55	47.81	71.4
City fuel economy=26.57 mpg				
Zone 3	1520	54.66	49.98	82.38
Zone 4	1578	106.83	50.02	68.66
Highway fuel economy=42.39 mpg				

Table 3.2: Simulation Matrix

Control Variable	Idle	Zone 1	Zone 2	Zone 3	Zone 4	Zone 5
IMOP	460, 475, 490, 505	455, 465, 475, 485	455, 465, 475, 485	455, 465, 475, 485	455, 465, 475, 485	455, 465, 475, 485
EMOP	230, 245, 260, 275	235, 245, 255, 265, 275, 285	235, 245, 255, 265, 275, 285	235, 245, 255, 265, 275, 285	235, 245, 255, 265, 275, 285	235, 245, 255, 265, 275, 285
Compression Ratio	11.9, 14.5, 17	11.9, 14.5, 17	11.9, 14.5, 17	11.9, 14.5, 17	11.9, 14.5, 17	11.9, 14.5, 17
CA50	8.5	10, 15	10, 15	10, 15	10, 15	10, 15
Ethanol Fraction	0.1, 0.2	0.1, 0.2, 0.85	0.1, 0.2, 0.85	0.1, 0.2, 0.85	0.1, 0.2, 0.85	0.1, 0.2, 0.85

Chapter 4 Results and Discussion

4.1 Overview

The simulation matrix was divided into five regions as discussed in Section 3.2.5. One region is the idle zone, while the others are medium to high load regions. The results of the GT-POWER simulations at these five regions or operating points will be discussed in detail in this chapter.

It is worth mentioning that constrained optimization was performed to limit the knock intensities and residual gas fractions to within allowable limits. The knock intensity limit was determined to be 600 units, as discussed in Section 3.2.3. The residual gas fraction limit was determined to be 30% by mass, based on engine fundamentals [8]. The results that did not lie within the allowable limits of knock and residual gas fraction were not considered during the optimization studies, and therefore are not discussed. The idle zone results will be discussed last as an understanding of the results of other zones will aid in the explanation of the trends seen during idle.

4.2 Results

It was observed that the engine responds to partial and full loads differently than it does to the idle load. Hence the discussion of the results has been broken down into two parts. First the simulation results at part loads will be discussed. The simulation matrix has four part load points from which the results of the 106.83 N·m torque point will be discussed in detail. The dependence of BSFC of the LAF engine on compression ratio, ethanol fraction, and VVT will be discussed. Moreover, the variation of knock intensities with VVT will also be shown.

4.2.1 Zone 4 results

Effect of VVT: The zone 4 operating point has an engine speed of 1578 RPM and brake torque value of 106.83 N·m. It is the point of high load and medium speed and hence representative of highway driving conditions. Understanding how different engine variables like compression ratio, VVT, or ethanol fraction affect the engine performance at this load point depends upon a clear understanding of the numbers and an analysis of the exhibited trends. Proper displays of the variables using graphs is an effective method to quickly understand the numbers and analyze the trends. For this purpose a set of plots will be used to present the results and support the discussion.

Figure 4.1 shows the dependence of BSFC and knock intensities on VVT. The blue line in Figure 4.1b shows the knock constraint. For a compression ratio of 11.9 and 10% ethanol, at every EMOP value BSFC increases as IMOP is increased except at a value of 235 EMOP. At 235 EMOP, the BSFC drops with increases in IMOP. An increase in IMOP means delayed intake valve closing. The reason for this behavior is that with delayed intake valve closing the effective compression ratio of the engine decreases. This decrease in effective compression ratio decreases the pressure and temperature at the end of the compression stroke, and hence a larger amount of fuel needs to be injected to achieve the target value of load or brake torque.

At a given IMOP value, increasing EMOP from 235 to 275 decreases the BSFC, but for an EMOP value of 285 the trend seems to reverse. It would be premature to comment on the results at EMOP values greater than 285 because of the unavailability of results. Nevertheless, it is known that there is always an optimum value of EMOP that gives the highest engine efficiency. This is because there is always a trade off involved in selecting the optimum value of EMOP. An increase in EMOP corresponds to late exhaust valve opening and closing. The late exhaust valve opening increases the available expansion ratio, and hence increases the work output of the engine. This may be the reason that the engine needs less fuel to target the same load because of the increased engine output. It

has to be kept in mind that opening the exhaust valve very late in the cycle can have an adverse effect on the efficiency of the engine. This is because a later exhaust valve opening decreases the engine blow down, and the engine has to do more work during the exhaust stroke to push the exhaust gases out of the combustion chamber decreasing the overall engine output. Based on these results, it is safe to conclude that the optimum value of EMOP lies somewhere close to 275 at a load of 106.83 N·m, a compression ratio of 11.9, 10% ethanol, and a CA50 of 10° ATDC.

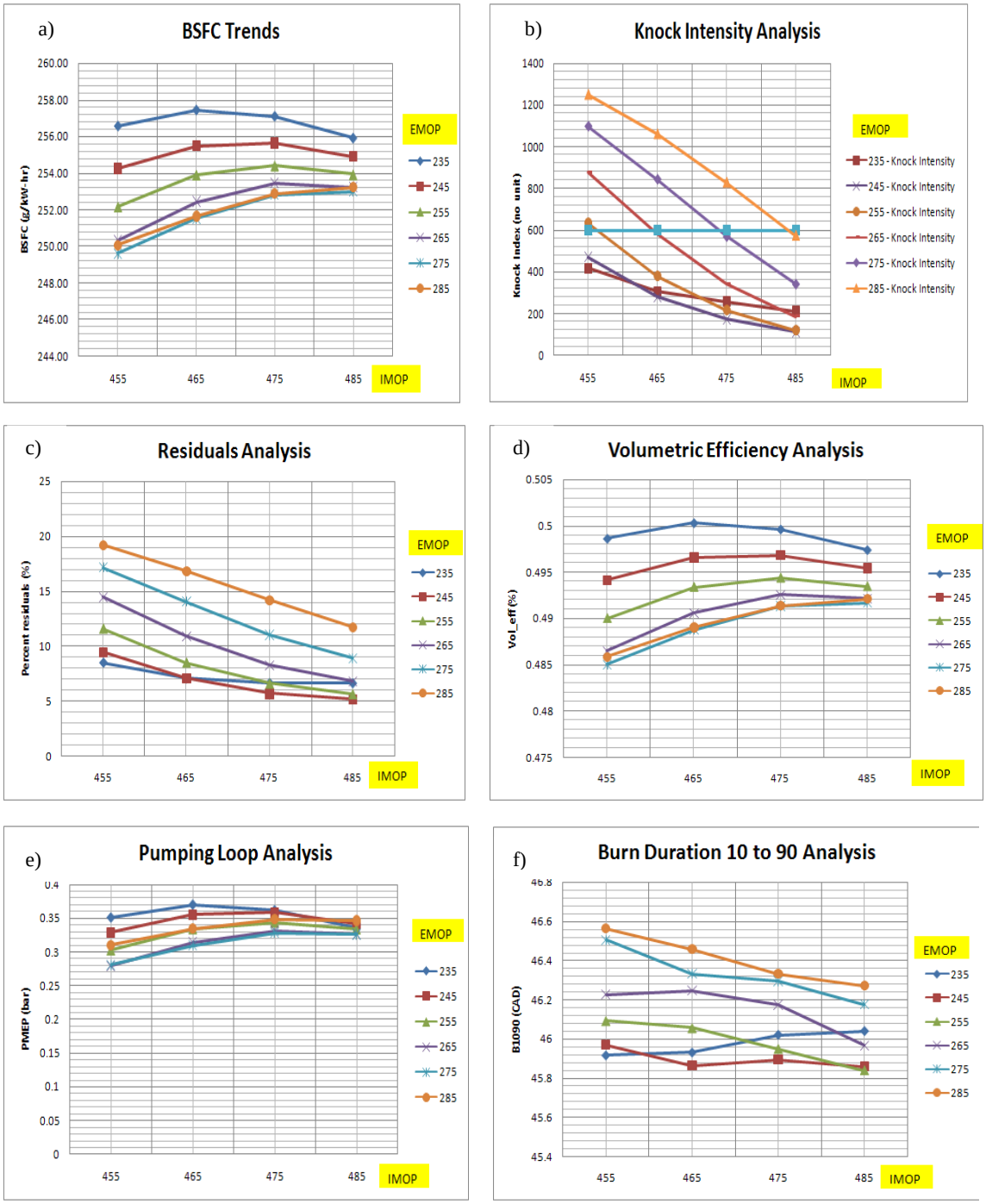

Figure 4.1: Dependence of a) BSFC, b) Knock Intensity, c) Residual Fraction, d) Volumetric Efficiency, e) PMEP, and f) Burn Duration 10 to 90 on VVT for zone 4, compression ratio 11.9, 10% ethanol and CA50 of 10 ATDC.

Although engine BSFC is of prime interest in deciding the values of the engine control variables, we have to limit quantities such as knock and residual fraction as well. As shown in Figure 4.1 running the LAF engine at EMOP greater than 265 may be detrimental due to higher knock intensities at these points. It can be seen that an increase in the EMOP value increases the knock intensities. The knock intensities are not directly affected by exhaust valve timing. Nevertheless, knock is highly dependent upon the temperature of air inducted during the intake stroke, which in turn is affected by the exhaust valve timing. If we analyze the effect of EMOP on residual gas fraction, we see that increased EMOP, or later exhaust valve closing, increases the residuals due to the increased overlap between intake and exhaust valve. The residuals increase the pressure and temperature of the inducted air, and in turn the tendency of the engine to knock increases.

The increase in IMOP decreases the knock intensities due to a decreased effective compression ratio. The lower the effective compression ratio, the lower are the temperature and pressure at the end of the compression stroke, which results in lower knock tendency. Moreover, an increase in IMOP value also reduces the residuals because of less valve overlap. Any increase in IMOP increases the volumetric efficiency and PMEP up to an IMOP value of 475, beyond which the trend seems to reverse. The reason for this behavior is that lower IMOP, or early intake valve opening, reduces the work required to induct fresh air charge into the cylinder. This happens because at medium to high engine speeds the air acquires high momentum while passing through the engine intake manifold. Opening the intake early utilizes this air momentum to fill the cylinder with fresh charge. Moreover, there is also a second phenomenon that indirectly affects the pumping work required. At a given EMOP, early opening of intake or lower IMOP value, means greater residuals. Some fraction of these residuals flows back into the intake manifold because of the pressure differential that exists between the exhaust manifold and the intake manifold. This reverse flow of exhaust into the intake manifold increases the manifold pressure, and provides faster filling of the cylinder with fresh air charge in the subsequent intake stroke. The higher EMOP value, or late closing of the

exhaust valve, increases the intake manifold pressure due to back flow of gases as explained earlier. This increases the intake air temperature and reduces the density, which causes volumetric efficiency to drop. Although late exhaust valve closing decreases volumetric efficiency till EMOP of 275, the trend seems to be reverse beyond this value.

The analysis of burn duration 10 to 90 is not solely dependent on VVT. Although the flow field in the cylinder is affected by VVT to a great extent, it is not the only independent variable that affects the burn duration. The spark timing, mixture entrainment, spark and injector location, and spray characteristics and many other variables are responsible for changes in burn duration. Though increases in EMOP seem to be increasing with burn duration 10 to 90, the reasons may not be limited solely to the changes in EMOP. The burn duration phenomenon is so complex that it is advisable to further analyze the burn process with CFD tools to determine its dependence on engine variables.

Effect of Compression Ratio: The compression ratio directly affects the efficiency of the engine. So increasing the compression ratio of the engine is always advisable provided that knock remains within acceptable limits. Figure 4.2 shows the effect of increasing the compression ratio on the efficiency of the engine and knock tendency. The results show a much expected trend in that although the engine is operating at much higher efficiency, the engine becomes more prone to knock until a point at which knock cannot be avoided by changing EMOP and IMOP timings. As shown in Figure 4.2 the entire VVT range is an inoperable zone, and the engine cannot be operated at this compression ratio even though it is desirable.

The increase in compression ratio also increases the residuals by a small amount. The reason is that at a higher compression ratio, the pressure at the end of expansion stroke is higher, which also increases the exhaust manifold pressure. During the subsequent intake

stroke there will be a greater reverse flow of exhaust gases to the intake manifold and cylinder due to a greater pressure differential.

The increase in compression ratio also seems to be increasing the PMEP and decreasing the volumetric efficiency of the engine. As described earlier, at higher compression ratios the pressure in the cylinder at the end of expansion stroke is greater. Thus the piston has to do extra work to push the exhaust out of the cylinder. Moreover, the vacuum condition before the start of the intake stroke helps to induct the fresh air charge. Since it is possible that cylinder pressure just before the intake stroke may be greater at higher compression ratios, the piston will have to do more work to induct the air. Therefore, the higher compression ratio may be increasing the PMEP and decreasing the volumetric efficiency of the engine.

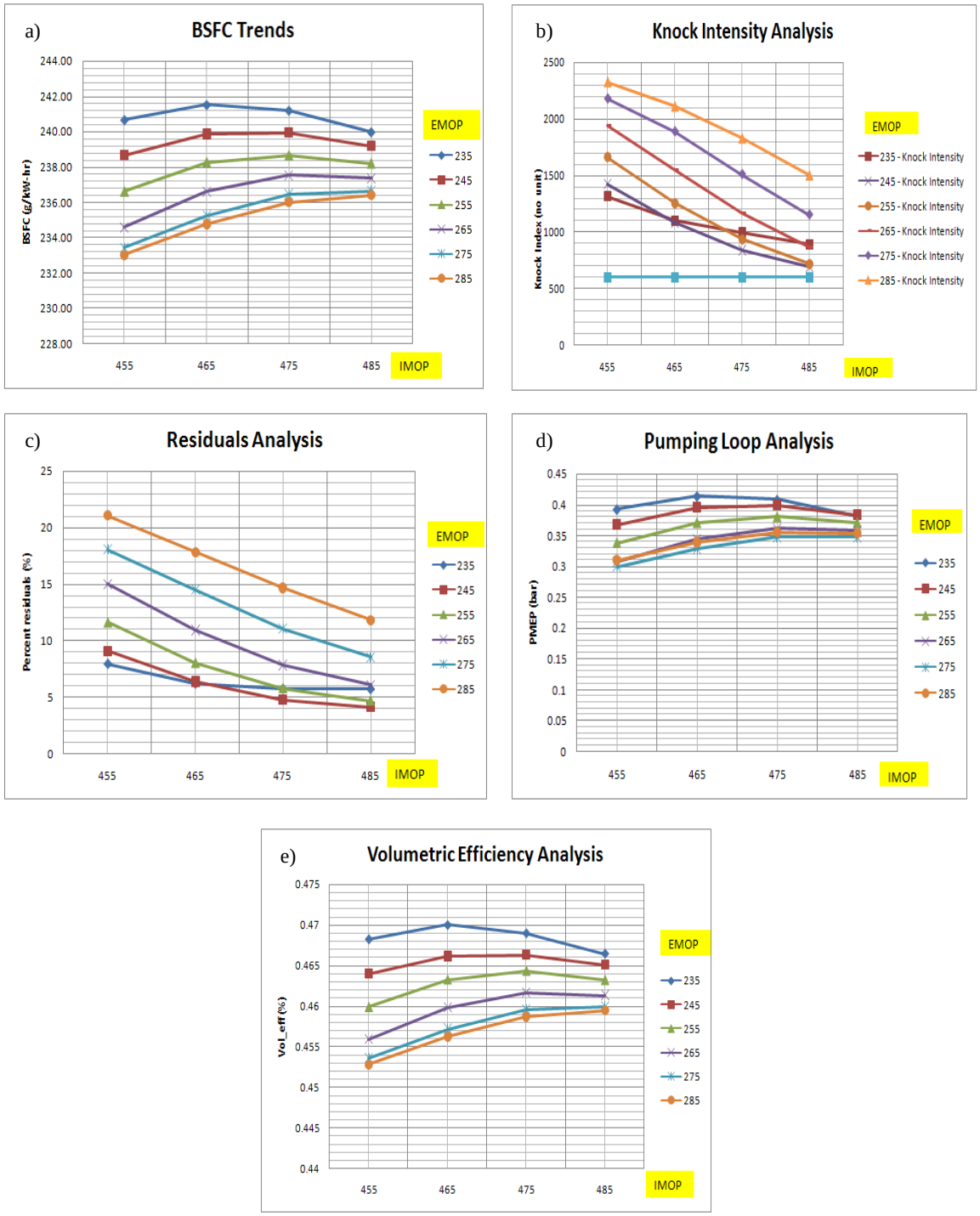

Figure 4.2: Dependence of a) BSFC, b) Knock Intensity, c) Residual Fraction, d) PMEP, and e) Volumetric Efficiency on VVT for Zone 4, Compression Ratio 17, 10% Ethanol and CA50 of 10 ATDC.

Effect of Ethanol addition: Ethanol has a lower heating value and higher heat of vaporization than gasoline. The lower heating value of ethanol results in a higher BSFC, which is as expected and observed by others. The higher octane number of ethanol helps to decrease the knock intensities, which is again an expected behavior.

Another effect of ethanol addition, which goes sometimes unnoticed, is an increase in the volumetric efficiency of the engine. The higher heat of vaporization of ethanol cools the incoming air due to heat transfer. As the air is cooled, its density is increased providing a larger available mass of air. The increase in the volumetric efficiency is also reflected in a decrease in pumping work, which can be seen from the PMEP graph in Figure 4.3.

Another important aspect of ethanol addition is that it decreases the burn duration, which can be seen from Figure 4.3. The reason is that ethanol has a lower laminar flame speed than pure gasoline, and hence it slows the burning process.

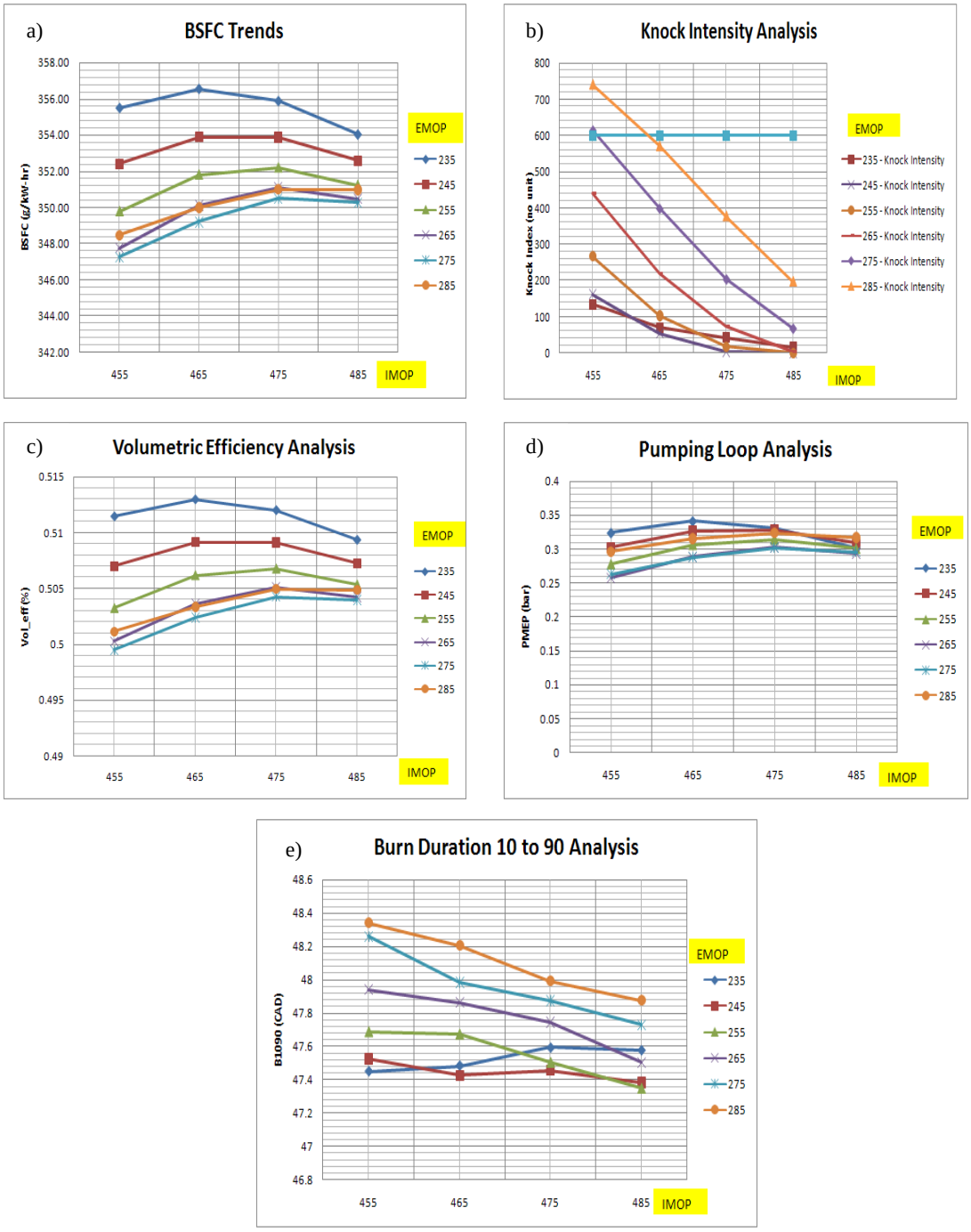

Figure 4.3: Dependence of a) BSFC, b) Knock Intensity, c) Volumetric Efficiency, d) PMEP, and e) Burn Duration 10 to 90 on VVT for Zone 4, Compression Ratio 11.9, 85% Ethanol and CA50 of 10 ATDC.

4.2.2 Zone 2 results

The results for zone 2 are shown in Figure 4.4. The torque and speed at zone 2 are 90.55 N·m and 1814 RPM, respectively. Comparing the results at zone 4 and zone 2 it can be easily seen that the trends in the engine variables such as BSFC, knock intensity, residual gas fraction, volumetric efficiency, PMEP and burn duration are similar. The engine parameters such as compression ratio, ethanol fraction, and VVT affect the engine performance at zone 2 in the same way as in zone 4. Hence explanation of these trends will not be given here to avoid repetition. Some key points are worth mentioning to summarize the analysis of engine performance at zone 2.

1) Early exhaust valve opening/closing increases BSFC although it decreases the knock intensity. Hence, the optimum value of EMOP is a trade-off between knock and engine efficiency.
2) Early intake valve opening/closing decreases BSFC while increasing the knock intensity. Therefore, the optimum value of IMOP is a trade-off between knock and engine efficiency.
3) Increasing the compression ratio decreases the BSFC although it makes the engine more prone to knocking due to increased knock intensity.
4) Ethanol addition in pure gasoline decreases the knock intensity enabling the goal of higher compression to be realized.

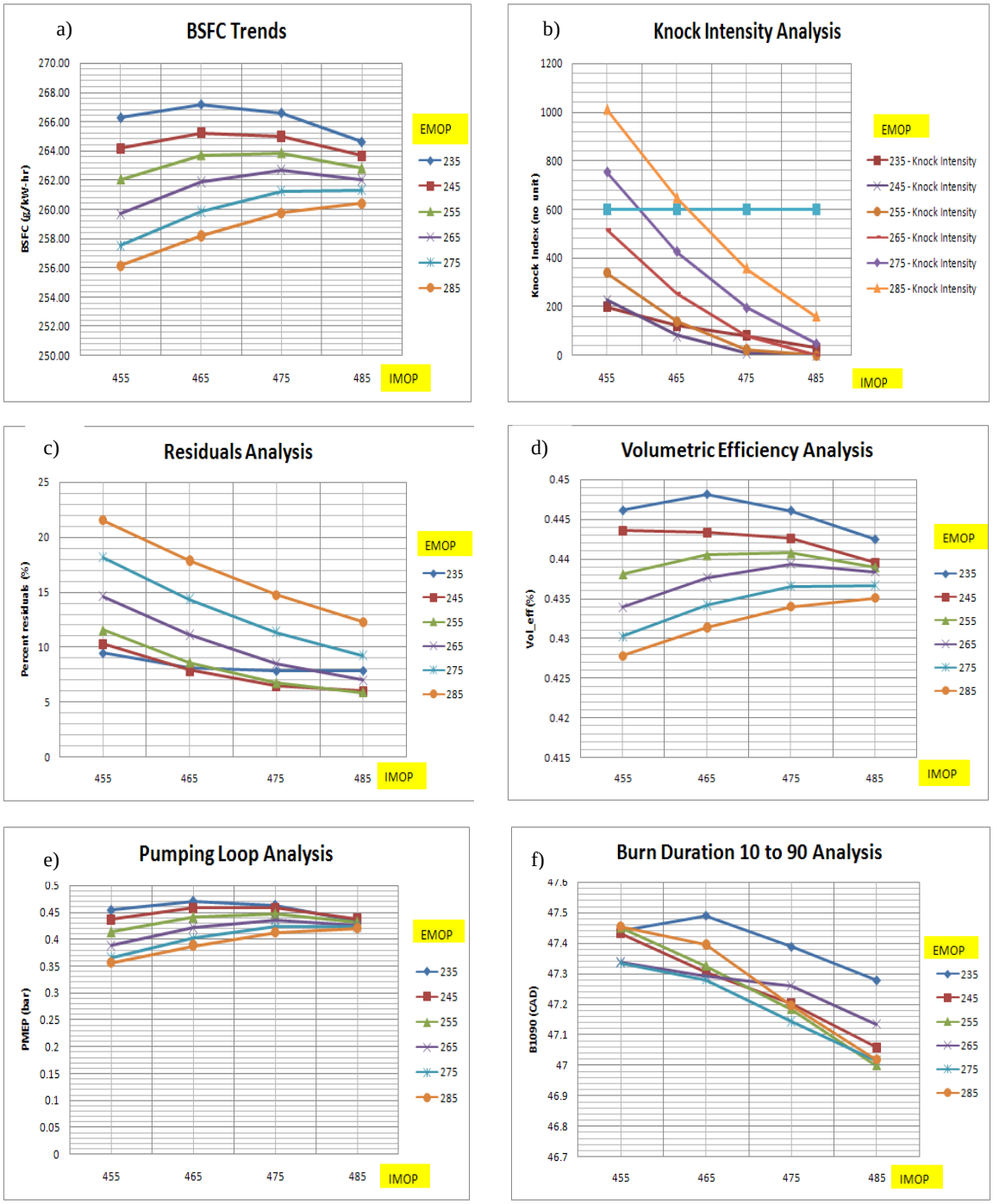

Figure 4.4: Dependence of a) BSFC, b) Knock Intensity, c) Residual Fraction, d) Volumetric Efficiency, e) PMEP, and f) Burn Duration 10 to 90 on VVT for Zone 2, Compression Ratio 11.9, 10% Ethanol and CA50 of 10 ATDC.

4.2.3 Idle zone results

The VVT affects the BSFC, residual gas fraction, PMEP, volumetric efficiency, and burn duration at the idle point in the same way it does at the torque point of 106.83 N·m. Hence the discussion of the results is the same and will not be repeated here. The interesting aspect of the results would be a comparison with the torque point of 106.83 N·m.

Although the trend of engine variables like BSFC at the idle point closely resembles the trends observed at the high load point, the magnitudes are quite different. The BSFC at idle point is much higher due in part to the incomplete combustion of the mixture. The breathing of the engine is affected adversely at the idle point because of low engine speed and the throttling of air in the throttle connection at low load. The poor breathing of the engine adds to the incomplete combustion of the fuel, and hence lower heat release. Therefore, more fuel has to be added to meet the target load. This can be seen from the results shown in Figure 4.5. The volumetric efficiency and PMEP plots in Figure 4.5 show how poorly the engine breathes at idle load points.

The level of residuals at the idle point is much higher than at high load points. This behavior is also expected as the pressure differential between the exhaust manifold and intake manifold is very high at the idle point.

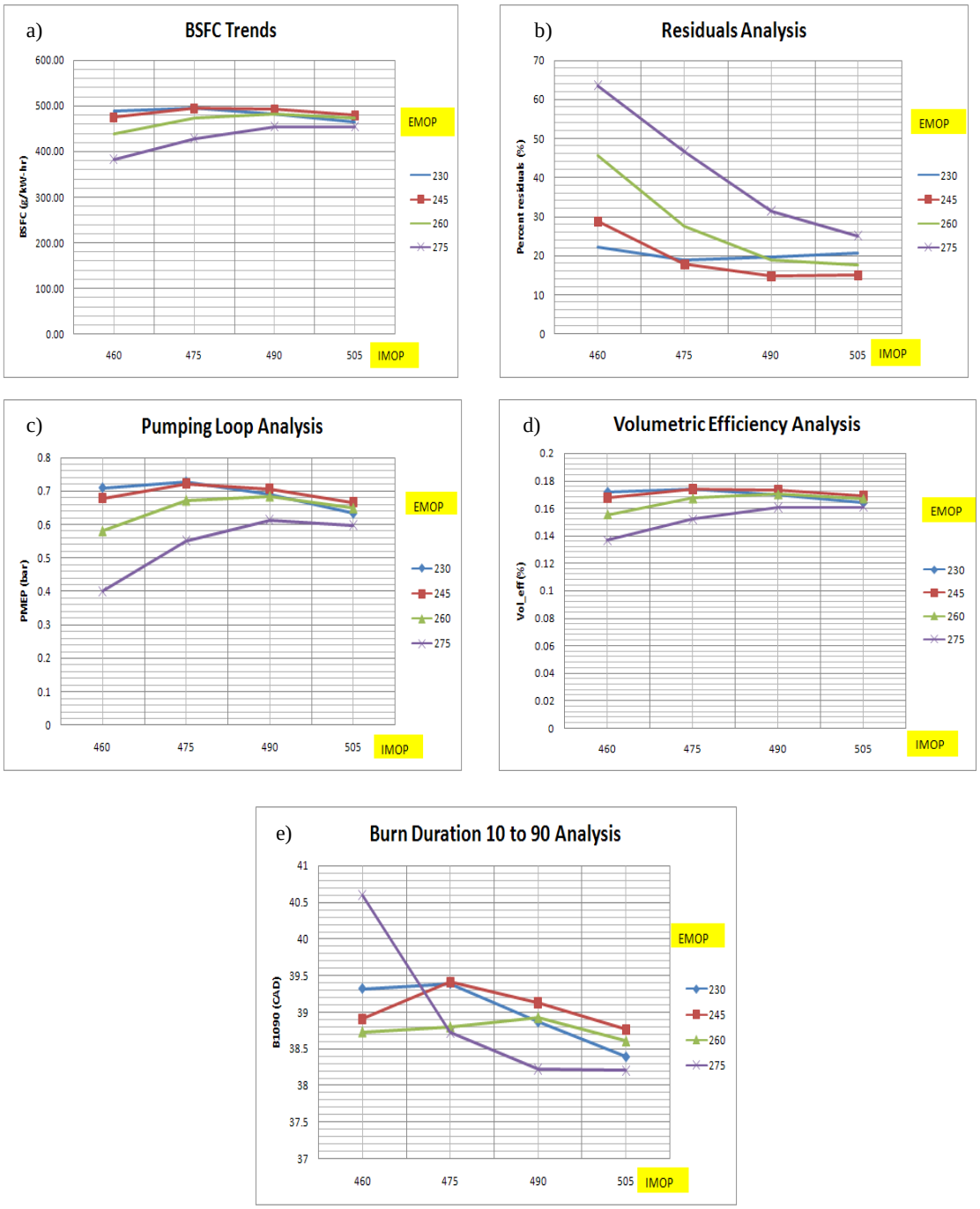

Figure 4.5: Dependence of a) BSFC, b) Knock Intensity, c) Residual Fraction, d) Volumetric Efficiency, e) PMEP, and f) Burn Duration 10 to 90 on VVT for Idle Zone, Compression Ratio 11.9, 10% Ethanol and CA50 of 8.5 ATDC.

4.2.4 BSFC correlations

This report was divided into two parts. First analyzed the trade offs of VVT, compression ratio, and ethanol fraction by studying their effect on engine BSFC, knock tendency, residuals percentage, volumetric efficiency, PMEP, and burn durations. The second part is correlating BSFC to engine variables that can be controlled, and hence can be used to adjust the BSFC around a certain desirable value, and would also help test engineers to run fewer tests by predicting BSFCs prior to running the tests. This subsection shows the BSFC correlation calculated at each load point using the engine variables that are independent and manually controllable.

BSFC correlation at Zone 1: Two different correlations are fitted for CA50 of 10 and 15 ATDC at each load point. Table 4.1 summarizes the values of the coefficients at each load point. The general form of the equation that is fitted at each load point is shown by Equation 4.1.

$$BSFC = (\text{Constant})\left[\frac{LHV_{\text{simulated fuel}}}{LHV_{\text{reference fuel}}}\right]^{(\text{coeff}_1)} \left[\frac{\text{Heat of vaporization}_{\text{simulated fuel}}}{\text{Heat of vaporization}_{\text{reference fuel}}}\right]^{(\text{coeff}_2)} \left[IVO_{simulation} - IVO_{ideal}\right]^{(\text{coeff}_3)} \left[EVO_{simulation} - EVO_{ideal}\right]^{(\text{coeff}_4)} \left[CR\right]^{(\text{coeff}_5)} [\text{Spark timing BTC}]^{(\text{coeff}_6)} \quad [4.1]$$

Table 4.1: Matrix of correlation coefficients

Brake Torque Nm	CA50 (ATDC)	Constant	$Coeff_1$	$Coeff_2$	$Coeff_3$	$Coeff_4$	$Coeff_5$	$Coeff_6$	R^2
19.05 (Idle)	8.5	6.1253	-1.0975	-0.0755	0.0529	0.0537	0.6699	0.6511	0.9658
28.05 (zone 1)	15	407.0088	-1.0805	-0.0574	0.0376	0.0464	-0.1635	0	0.996
28.05 (zone 1)	10	408.6032	-1.0629	-0.0497	0.0346	0.0447	-0.1569	0	0.996
90.55 (zone 2)	15	376.6501	-0.9818	-0.0059	0.0085	0.0167	-0.197	0	0.9978
90.55 (zone 2)	10	385.615	-0.9009	0.0323	0.0037	0.0151	-0.1983	0	0.9986
54.66 (zone 3)	15	338.9331	-0.9971	-0.0202	0.0297	0.0329	-0.1614	0	0.9982
54.66 (zone 3)	10	345.1799	-0.9798	-0.0127	0.0221	0.0307	-0.1528	0	0.9984
106.83 (zone 4)	15	365.8139	-0.9854	-0.013	0.0061	0.0115	-0.1874	0	0.999
106.83 (zone 4)	10	381.1371	-0.9685	-0.0044	0.0018	0.0094	-0.1947	0	0.9992

The fitted values can be graphically compared to the simulated values. This graphical comparison is avoided here as it would require an addition of 9 more plots for each equation in the Table 4.1. Hence the R^2 terms are added in the Table 4.1 that compare the fitted and simulated values numerically. The higher value of R^2 corresponds to a better fit. Values very close to 1 signify that the variance between fitted and simulated values of BSFC is negligibly small and the fitting function gives a good approximation to the BSFC.

Note: EVO_{ideal} and IVO_{ideal} in the above equation are considered to be BDC and TDC positions respectively.

Physical significance of LHV and compression ratio coefficient: The addition of ethanol increases the BSFC of the engine as shown and discussed earlier. The BSFC evaluates the performance of the engine on a mass basis, and hence is not a true representation of engine efficiency. Ethanol has a lower heating value than gasoline, and therefore to achieve the same amount of heat release from both fuels a greater mass of ethanol is required. This means that to properly evaluate engine operation with two different fuels a common reference point is needed. Engine researchers have primarily used energy

release from the fuel as a reference to compare performance of an engine operating on two different fuels. This type of comparison focuses on calculating the fuel consumption required to achieve the same amount of energy release. The fuel consumption is a quantity with units of g/kW-hr, which shows that it does not compare equivalent input and output. By observing the units of fuel consumption, one can interpret that the input is mass of fuel and the output is energy. As discussed earlier, due to lower the heating value, the required input amount is higher for ethanol to produce the same amount of work. This gives an impression that ethanol performs poorly in terms of efficiency, which is not the case. The true representation of efficiency of the engine is comparing the energy given to the system with the work produced by the system. A modified form of engine efficiency is given by equation 4.2. Therefore, obviously for ethanol less energy is given to the engine per unit mass, and hence less work is produced by the engine, but if these two quantities are compared to each other a true idea of engine efficiency is obtained. Therefore, comparing the mass required with the work produced as in the case of BSFC, energy required with the work produced should be compared when evaluating performance of an engine operating on two different fuels.

Calculations at zone 4:

$$\eta_{engine} = \frac{1}{\mathrm{LHV}_{fuel} \times \mathrm{BSFC}} \qquad [4.2]$$

Using the BSFC correlation at zone 4 and CA50 of 10° ATDC in Equation 4.2 results in

$$\eta_{engine} = \frac{1}{\text{LHV\_simulated fuel} \times (381.1371)\left[\frac{LHV_{\text{simulated fuel}}}{LHV_{\text{reference fuel}}}\right]^{(-0.9685)} \left[\frac{\text{Heat of vaporization}_{\text{simulated fuel}}}{\text{Heat of vaporization}_{\text{reference fuel}}}\right]^{(-0.0044)} \left[IVO_{simulation} - IVO_{ideal}\right]^{(0.0018)} \left[EVO_{simulation} - EVO_{ideal}\right]^{(0.0094)} \left[CR\right]^{(-0.1947)} [\text{Spark timing BTC}]^{(0)}} \quad [4.3]$$

Assuming that,

$$X = (381.1371)\left[\frac{LHV_{\text{simulated fuel}}}{LHV_{\text{reference fuel}}}\right]^{(-0.9685)} \left[\frac{\text{Heat of vaporization}_{\text{simulated fuel}}}{\text{Heat of vaporization}_{\text{reference fuel}}}\right]^{(-0.0044)} \left[IVO_{simulation} - IVO_{ideal}\right]^{(0.0018)} \left[EVO_{simulation} - EVO_{ideal}\right]^{(0.0094)} \left[CR\right]^{(-0.1947)} [\text{Spark timing BTC}]^{(0)} \quad [4.4]$$

Means that Eqn. 4.3 reduces to ,

$$\eta_{engine} = \frac{1}{(\mathrm{LHV}_{\mathrm{sim\_fuel}}) \times \left[X \times \left[\frac{LHV_{\text{simulated fuel}}}{LHV_{\text{reference fuel}}} \right]^{(-0.9685)} \right]} \qquad [4.5]$$

Rearranging the terms results in

$$\eta_{engine} = \frac{1}{\left\{ \left[\mathrm{LHV}_{\text{reference fuel}} \times \frac{\mathrm{LHV}_{\text{simulated fuel}}}{\mathrm{LHV}_{\text{reference fuel}}} \right] \times \left[X \times \left[\frac{LHV_{\text{simulated fuel}}}{LHV_{\text{reference fuel}}} \right]^{(-0.9685)} \right] \right\}} \qquad [4.6]$$

$$\eta_{engine} \propto \frac{1}{\left\{ \left[\mathrm{LHV}_{\text{reference fuel}} \right] \times \left[\left[\frac{LHV_{\text{simulated fuel}}}{LHV_{\text{reference fuel}}} \right]^{(0.0315)} \right] \right\}} \qquad [4.7]$$

If the previous calculations are performed for pure ethanol as the simulated fuel and pure gasoline as a reference fuel then

$$\left[\frac{LHV_{\text{simulated fuel}}}{LHV_{\text{reference fuel}}} \right]^{(0.0315)} = (0.61)^{(0.0315)} = 0.9845 \qquad [4.8]$$

Therefore, in this case the efficiency will be affected by a factor 1/0.9854. This means the efficiency of the engine increases by a factor 0.0148 if pure ethanol is used instead of pure gasoline. To understand why the performance evaluation based on mass is incorrect and on energy correct, Figures 4.1 and 4.3 and Eqn. 4.8 need to be considered. Figures 4.1 and 4.3 indicate that if 85% ethanol is used instead of 10% ethanol then BSFC increases by 40% or a factor of 0.4, and at the same time Eqn. 4.8 shows that the efficiency of the engine increases by a factor of 0.0148 or approximately 1.5%.

All interested readers should refer to the Excel workbook in the MTU/ethanol directory for the plots of BSFC and other variables at each load point. The graphical comparison between the fitted and simulated values of BSFC can also be referred from the same workbook.

Chapter 5 Conclusions and Recommendations

5.1 Summary

The current study was performed using GT-POWER and a combustion compound model. It should be noted that any software used for modeling studies does a poor job of capturing transients and discontinuities, especially when predicting stochastic engine operation. However, based on the current study, the effects of compression ratio, ethanol, and VVT on engine performance parameters like BSFC, knock intensity, volumetric efficiency, PMEP and residual gas fraction can be well understood using the results of the simulations. The five point optimization can be used to determine if increases in compression ratio or ethanol content will be effective.

The objective of the current study was to observe the trends of BSFC with variations in ethanol content, compression ratio, and VVT, and give possible explanations for the observed trends. The following conclusions can be drawn from the current study. It is theoretically advisable to use a higher compression ratio to improve engine efficiency, but a detailed study might show insufficient improvement in engine efficiency with compression ratio. In the same way, there may be some unexpected occurrences with ethanol addition in the reference fuel, and hence advantages and disadvantages of these performance improvement strategies should be analyzed in detail before implementing them in engines. The functions fitted to BSFC at each zone/operating point will make it possible to use these results in mathematical models in future studies.

5.2 Conclusions

1) An increase in compression ratio results in a reduction in the BSFC due to an increase in thermodynamic efficiency, but there is little to no improvement in engine efficiency with an increase in compression ratio at low loads.
2) A higher compression ratio makes the useful VVT range narrower, and hence possible improvements in engine efficiency with use of wider a VVT range may be offset. For example, at a compression ratio of 17 almost the entire VVT range becomes ineffective and inoperable due to knock constraints, whereas at a compression ratio 11.9 the engine may run within acceptable knock limits for most of the VVT range.
3) Ethanol addition in the reference fuel increases the BSFC. This is because ethanol has a lower LHV, which requires more fuel to be injected to achieve the same torque.
4) Ethanol addition increases volumetric efficiency. This effect is caused by the higher heat of vaporization of ethanol fuel, which cools the incoming air due to heat transfer between the air and fuel.
5) In almost all cases, an early intake valve opening appears to be beneficial from an optimization of BSFC perspective, but early intake valve opening also increases the residual gas fraction, which can be detrimental to engine operation because of increased variability of the residual gas fraction.
6) The optimum EMOP depends on the trade-off between blow down gain and expansion work loss. This trade-off point changes with load and is not constant for the entire range of engine operation.
7) Though ethanol addition increases BSFC it affects the efficiency of the engine by a small but negligible amount and in some cases it actually increases efficiency instead of lowering it.

5.3 Future Work

The current study is innovative and reliable as the trends observed are sensible and in accordance with the literature. Nevertheless, there are possible improvements in the current study.

5.3.1 Model Improvements

1) The current model was built for the LAF engine and the burn duration correlation is valid only for this engine. As the engine to be analyzed changes, the burn duration correlations change, which makes it difficult to use the model as a truly predictive tool. Further analysis of combustion with CFD tools, chemical kinetics studies, and physical understanding of engine behavior to different operating variables might make the model truly predictive in nature, it can then be used with any engine model to acquire reliable results.
2) The GT-POWER knock model used in this particular study was formulated in 1978 and there has been much research conducted on knock since this time. Therefore a user-built model of knock can be used for better knock prediction.
3) The current model has no capability of analyzing transient response like cold start. A future modification can be performed to make the model capable of performing cold start studies.
4) Assembly of an entire integrated vehicle study with engine, powertrain, brakes, cooling and lubrication systems, different platforms in GT-POWER can be used. The vehicle model thus built can be run with different test cycles FTP or USDS for more real world modeling of the phenomenon.

5.3.2 Other Improvements

The use of a software in the loop system can be the greatest improvement to producing reliable and fast optimization results. Software in the loop systems are used in large industries and have proven to be effective. There are many algorithms on the market that have been developed for software in the loop optimization and the process can be automated. With such optimization techniques, engine studies will be less time consuming and laborious.

References

1. Renewable fuels association (RFA), "Ethanol Industry Statistics", http://www.ethanolrfa.org/pages/statistics#A, 2010.

2. Naber, J. , "Flex-Fuel Powertrain for Hybrid Applications through Combustion Optimization, Crank-Start Hydrocarbon Reduction, and Engine Simulation", MIEEG proposal, Case no. U13129, 2008.

3. Wright, N. , Drane, R. , "Using the Matlab Toolset to Improve Efficiency in the EOBD Calibration Process", presented at Mathworks International Automotive Conference, Stuttgart, June 15-16, 2004.

4. Saerens,B. , Vandersteen, J. , Persoons, T. , Swevers,J. , Deihl, M. , Van Den Bulck, E. , "Minimization of the fuel consumption of a gasoline engine using dynamic optimization", Applied Energy (86): 1582-1588, 2009.

5. "GT-SUITE Users Manual", GT-Suite (version 7.0), Gamma Technologies, Westmont, IL, 2010.

6. Yeliana, Y., "Parametric Combustion Modeling for Ethanol-Gasoline Fueled Spark Ignition Engines"PhD thesis, Mechanical Engineering Department, Michigan Technological University, Houghton, 2010.

7. Syed, I. Z., Yeliana, Y., "Numerical Investigation of Laminar Flame Speed of Gasoline - Ethanol/air mixtures with varying Pressure, Temperature and Dilution", SAE Technical Paper, 2010-01-0620, 2010.

8. Heywood, J., "Internal Combustion engine Fundamentals", McGraw-Hill Series in Engineering, ISBN 0-07-028637- X, 1988.

9. Rask, E., and Sellnau, M., "Simulation Based Engine Calibration: Tools, techniques and Applications", SAE Technical Paper 2004-01-1264, 2004.

10. Wu, B., Prucka, R., Filipi, Z., Kramer, D., Ohl, G., "Cam Phasing Optimization Using Artificial Neural Networks as Surrogate Models- Fuel Consumption and NOx Emissions", SAE Technical Paper 2006-01-1512, 2006.

11. Parvate-Patil, G. B., Hong, H., Gordon, B., "An Assessment of Intake and Exhaust Philosophies for Variable Valve Timing", SAE Technical Paper 2003-32-0078, 2003.

12. Bozza, F., Torella, E., "Use of 1D Cycle Simulations for A/F Control in VVT Engines", SAE Technical Paper 2003-01-0027, 2003.

13. Schwaderlapp, M., Habermann, K., Yapici, K., "Variable Compression Ratio- A Design Solution for Fuel Economy Concepts", SAE Technical Paper 2002-01-1103, 2002.

14. Nilsson, Y., Eriksson, L., Gunnarsson, M., "A Model for Fuel Optimal Control of a Spark Ignited Variable Compression Engine", SAE Technical Paper 2006-01-0399, 2006.

15. Naber, J., Blough, J., Frankowski, D., Goble, M., Szpytman, J., "Analysis of Combustion Knock metrics in Spark-Ignition Engines", SAE Technical Paper 2006-01-0400, 2006.

16. Wallner, T., Miers, S. A., "Combustion behavior of Gasoline and Gasoline/Ethanol Blends in a Modern Direct-Injection 4-Cylinder Engine", SAE Technical Paper 2008-01-0077, 2008.

17. Caton, P., Hamilton, L., Cowart, J., "An Experimental and Modeling Investigation into the Comparative Knock and Performance Characteristics of E85, Gasohol [E10]

and Regular Unleaded Gasoline [87(R+M)/2]", SAE Technical Paper 2007-01-0473, 2007.

18. Gish, R. E., McCullough, J. D., Retzloff, J. B., Mueller, H. T., "Determination of True Engine Friction" SAE Technical Paper 580063, 1958.

19. Rezeka, S. F., Henein, N. A., "A New Approach to Evaluate Instantaneous Frcition and Its Components in Internal Combustion Engines", SAE Technical Paper , 840179, 1984.

20. Matt Wiles, General Motors Corporation, personal communications, July, 2010.

21. Pipitone, E., "A New Simple Friction Model for S. I. Engine", SAE Technical Paper, 2009-01-1984, 2009.

22. Sethu, C., Leustek, M., Bohac, S., Filipi, Z., Assanis, D., "An Investigation in Measuring Crank Angle Resolved In-Cylinder Engine Friction Using Instantaneous IMEP Method", SAE Technical Paper 2007-01-3989, 2007.

23. Haskew, H. M., Liberty, T. F., McClement, D., "Fuel Permeation from Automotive Systems", presented at CARB (California Air Resources Board) Public Meeting, Sacramento, June 21, 2001. http://www.crcao.com/reports/recentstudies2004/E65%20Final%20Report%209%202%2004.pdf

24. Rouse, B., "Part Load Combustion Characterization of Ethanol-Gasoline Fuel Blends in a Single Cylinder Spark Ignition Direct Injection Variable Cam Timing Variable Compression Ratio Engine", M.S thesis, Mechanical Engineering

Department, Michigan Technological University, Houghton, 2009.

25. “MATLAB Users Guide”, MATLAB (version 10. a), Mathworks Inc, Natick, MA, 2010

Appendix A Sl_{ign} calculations

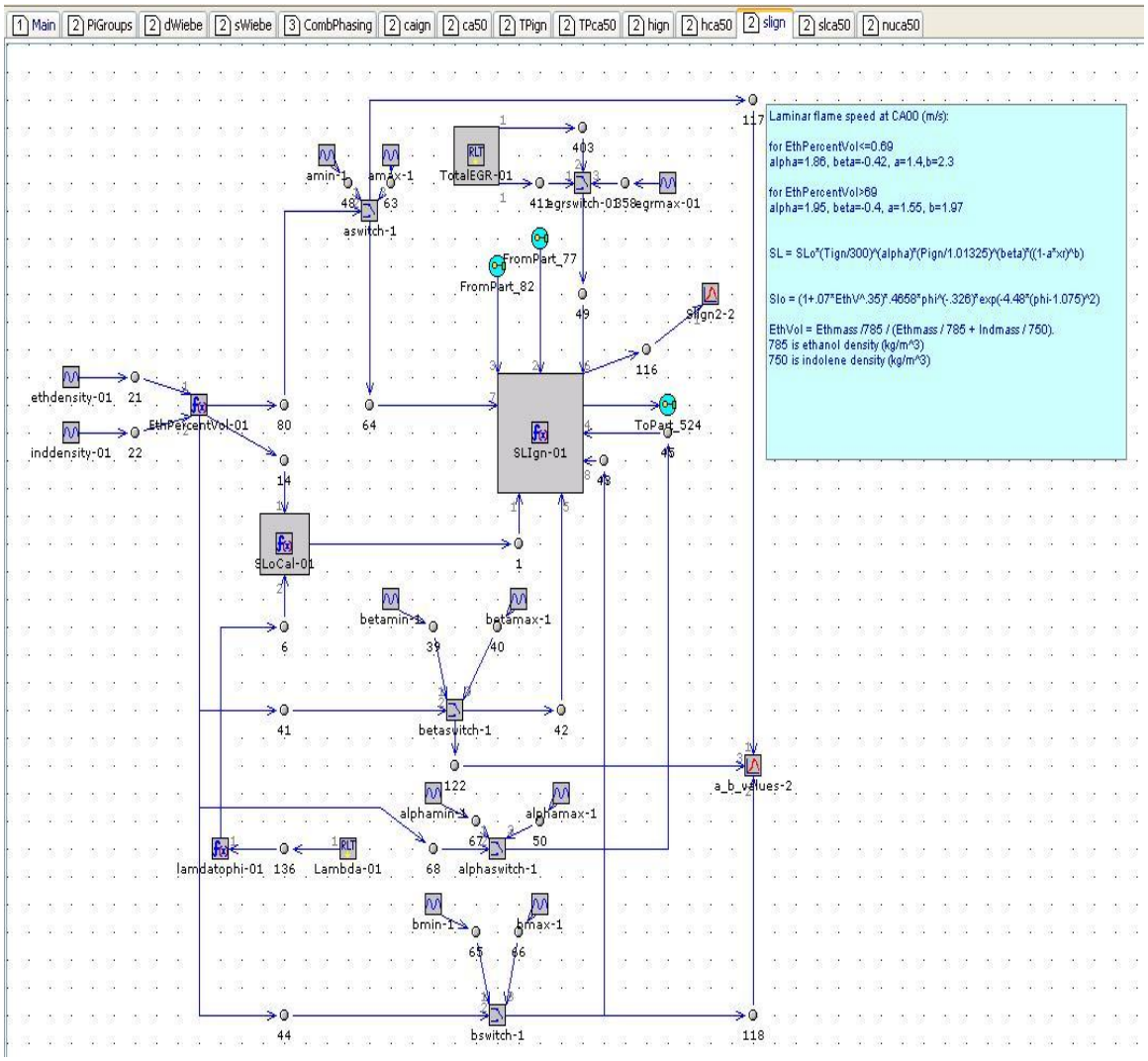

Updated laminar flame speed calculations at Ignition point (sl_{ign})

Appendix B Sl_{CA50} calculations

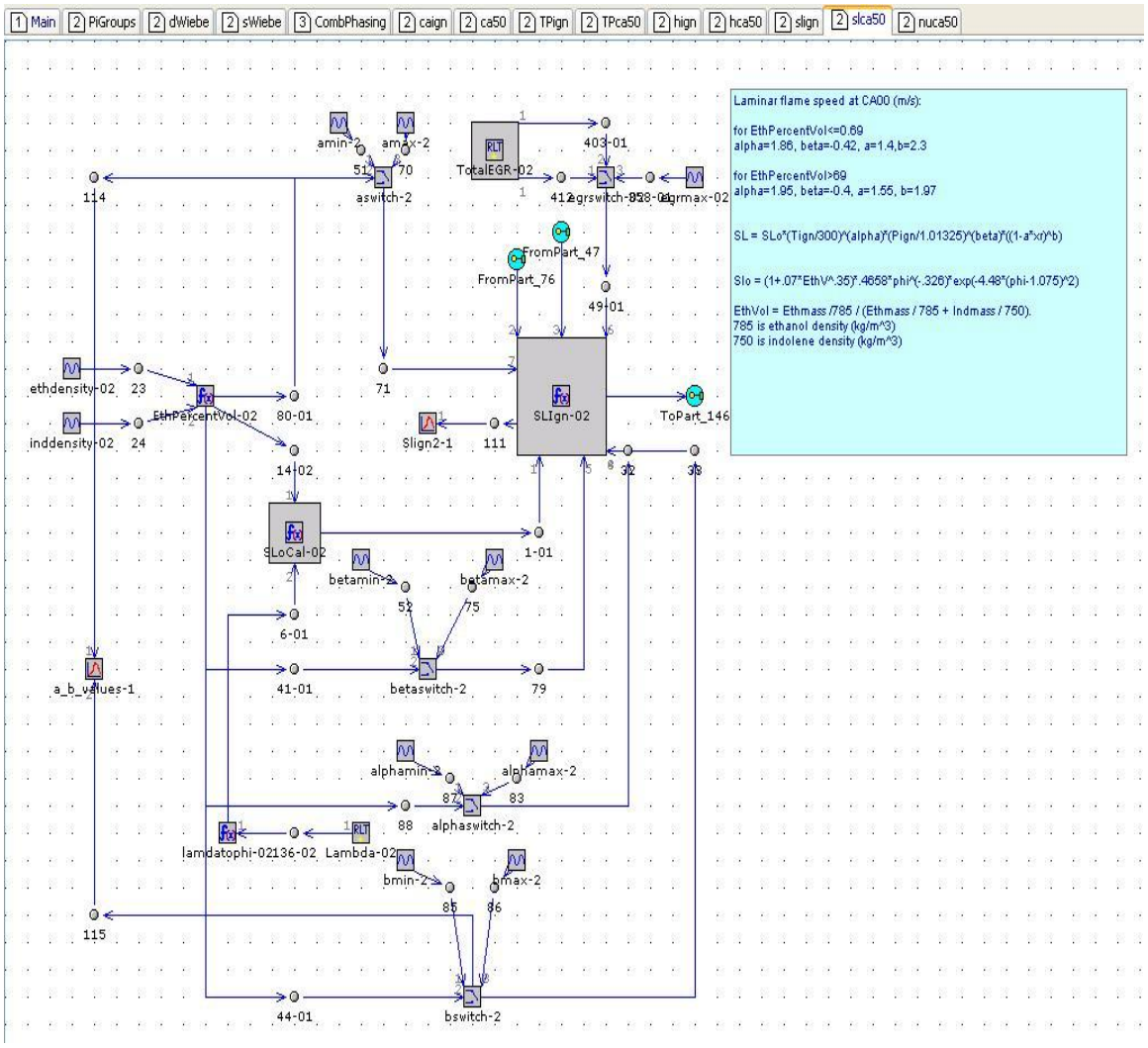

Updated laminar flame speed calculations at Ignition point (sl_{CA50})

Appendix C Knock model calibration at part load condition with EMOP= -97 and IMOP= 120

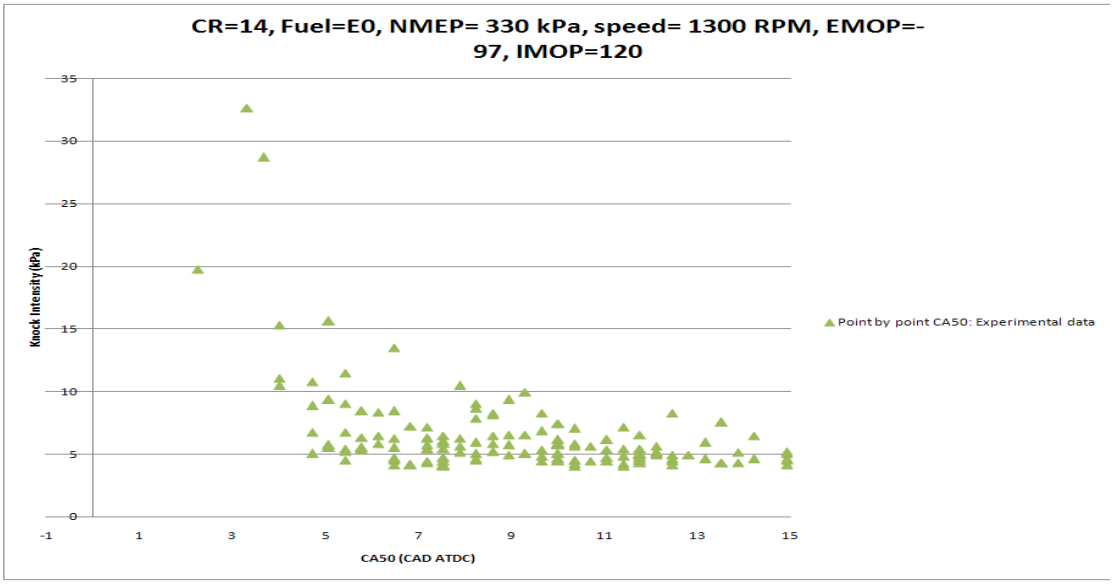

Experimental knock intensity variation with CA50

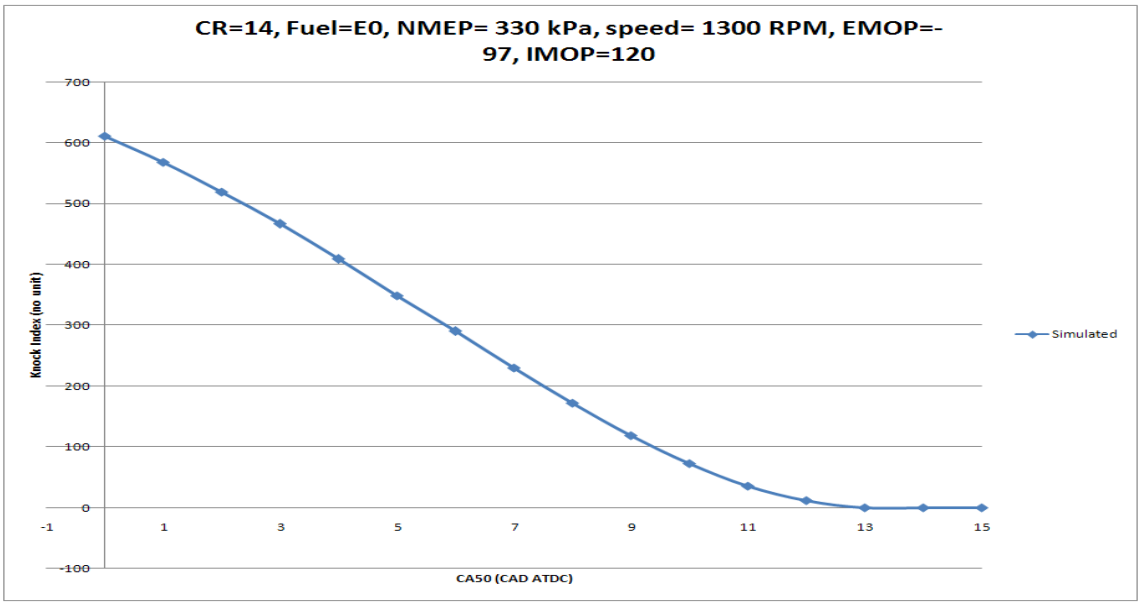

Simulated knock index variation with CA50

Appendix D Knock model calibration at part load condition with EMOP= -87 and IMOP= 120

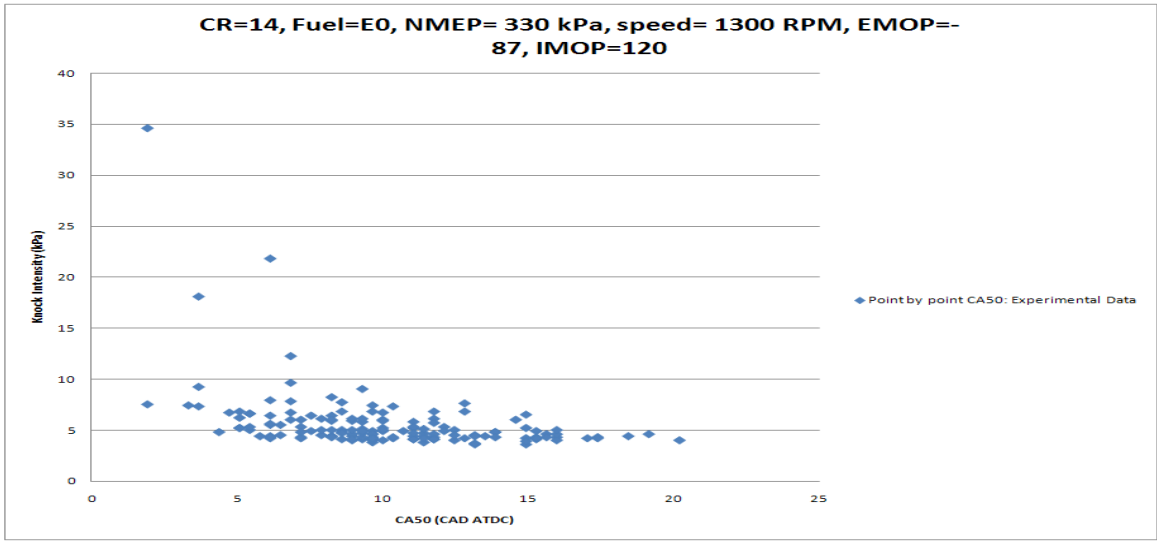

Experimental knock intensity variation with CA50

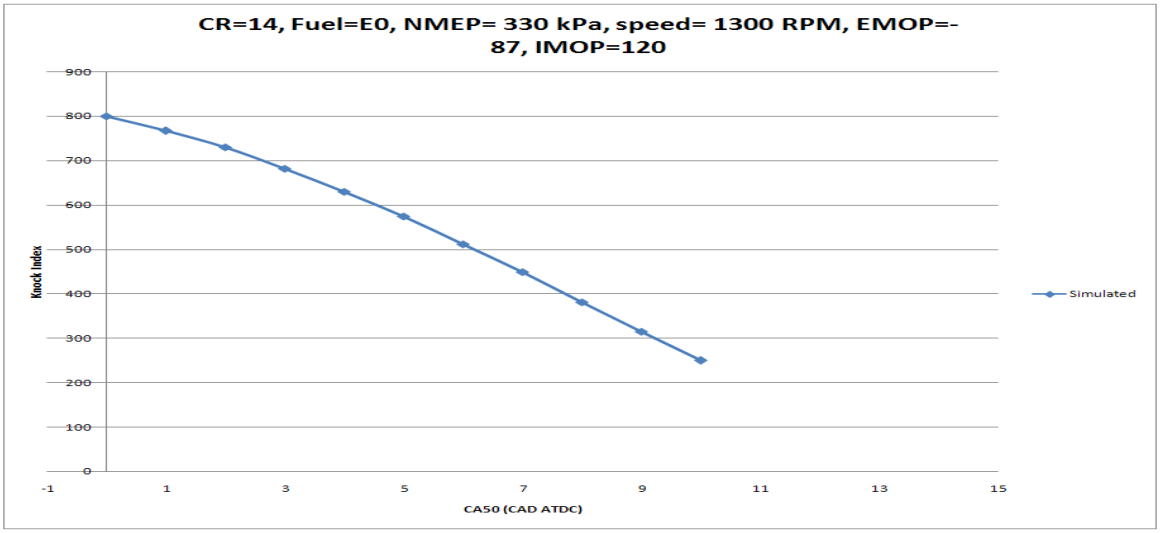

Simulated knock index variation with CA50

Appendix E Knock model calibration at part load condition with EMOP= -84 and IMOP= 120

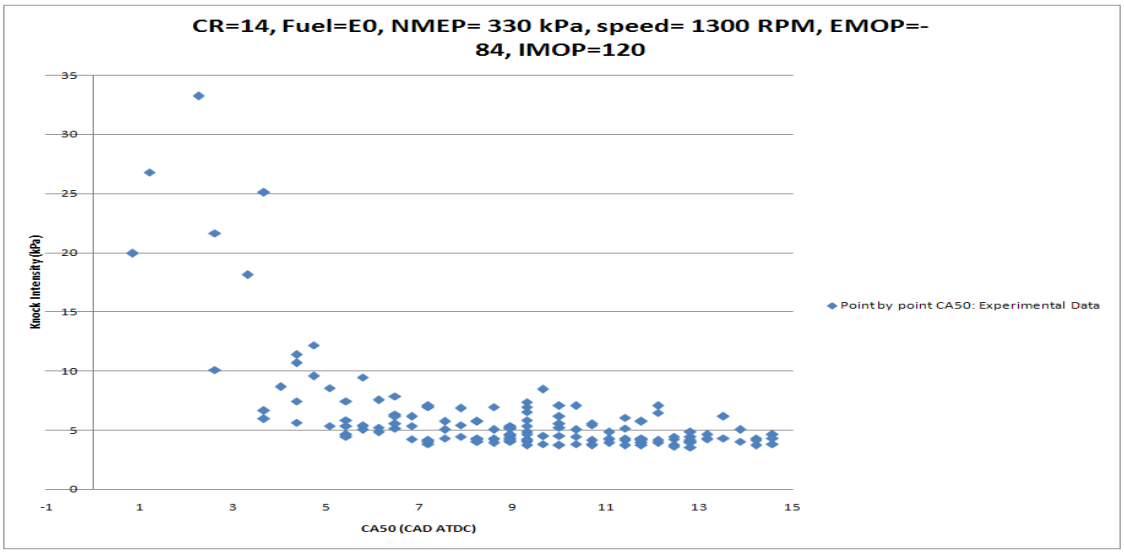

Experimental knock intensity variation with CA50

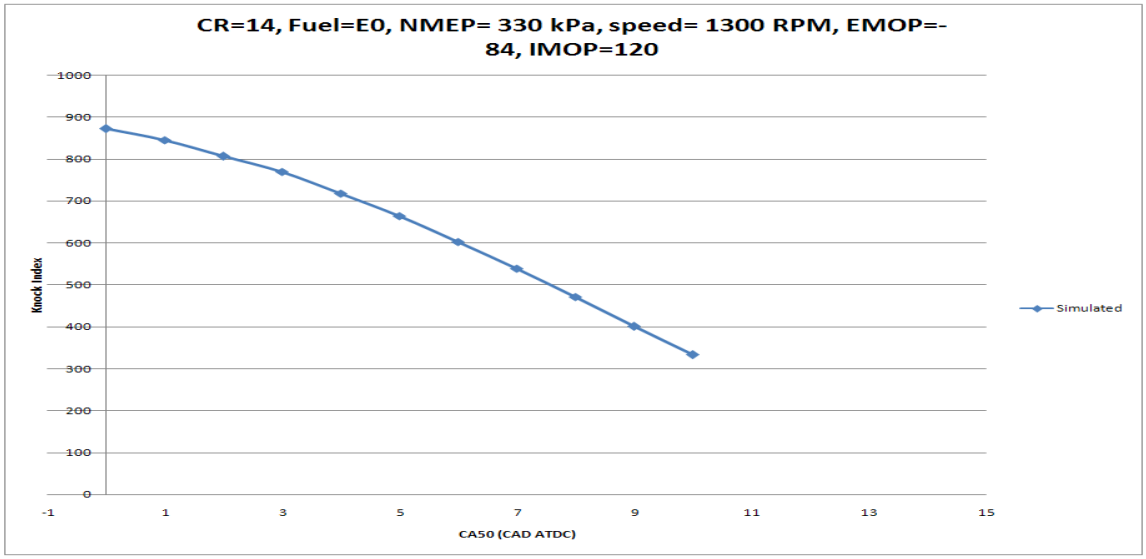

Simulated knock index variation with CA50

Appendix F h_{ign} calculations

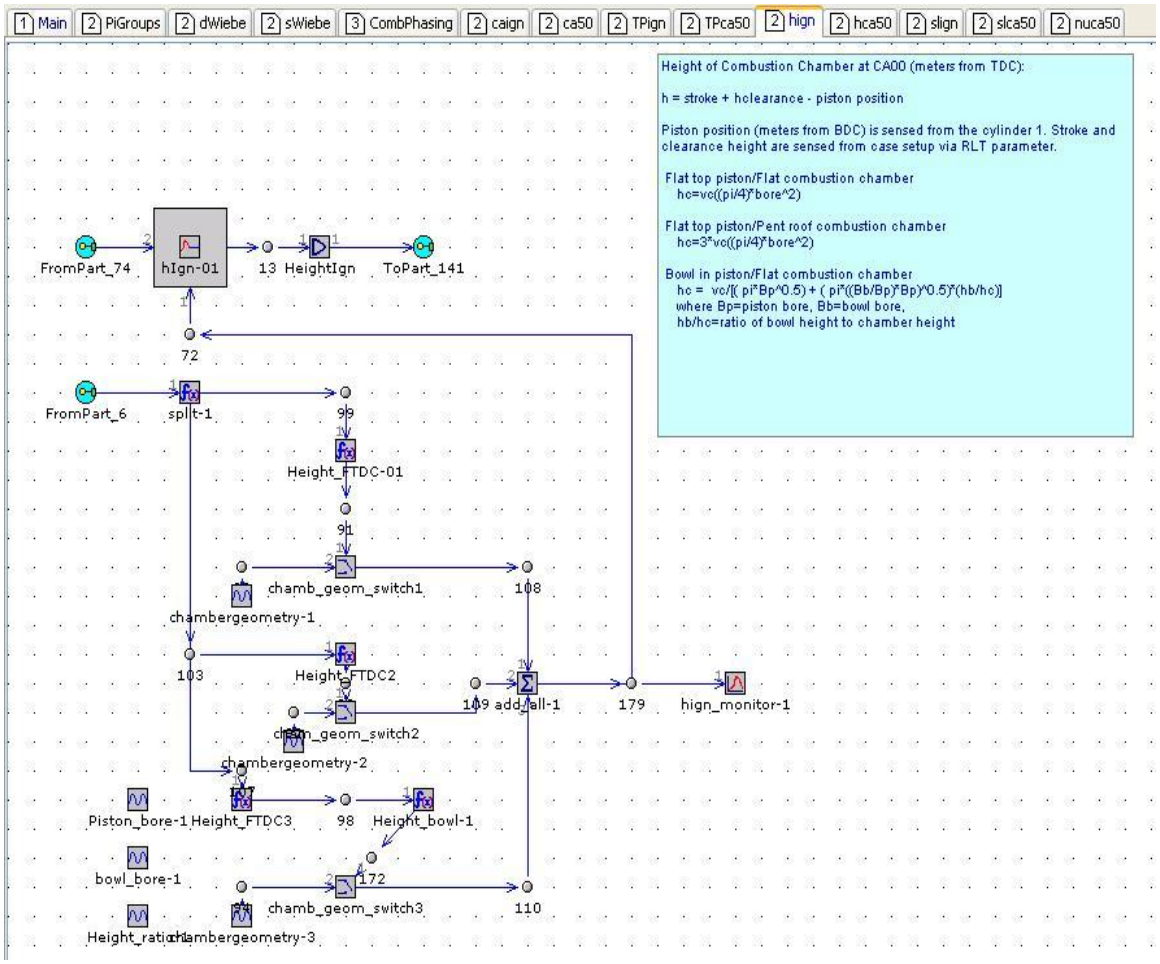

Updated clearance height calculations at ignition point (h_{ign})

Appendix G h_{ign} calculations

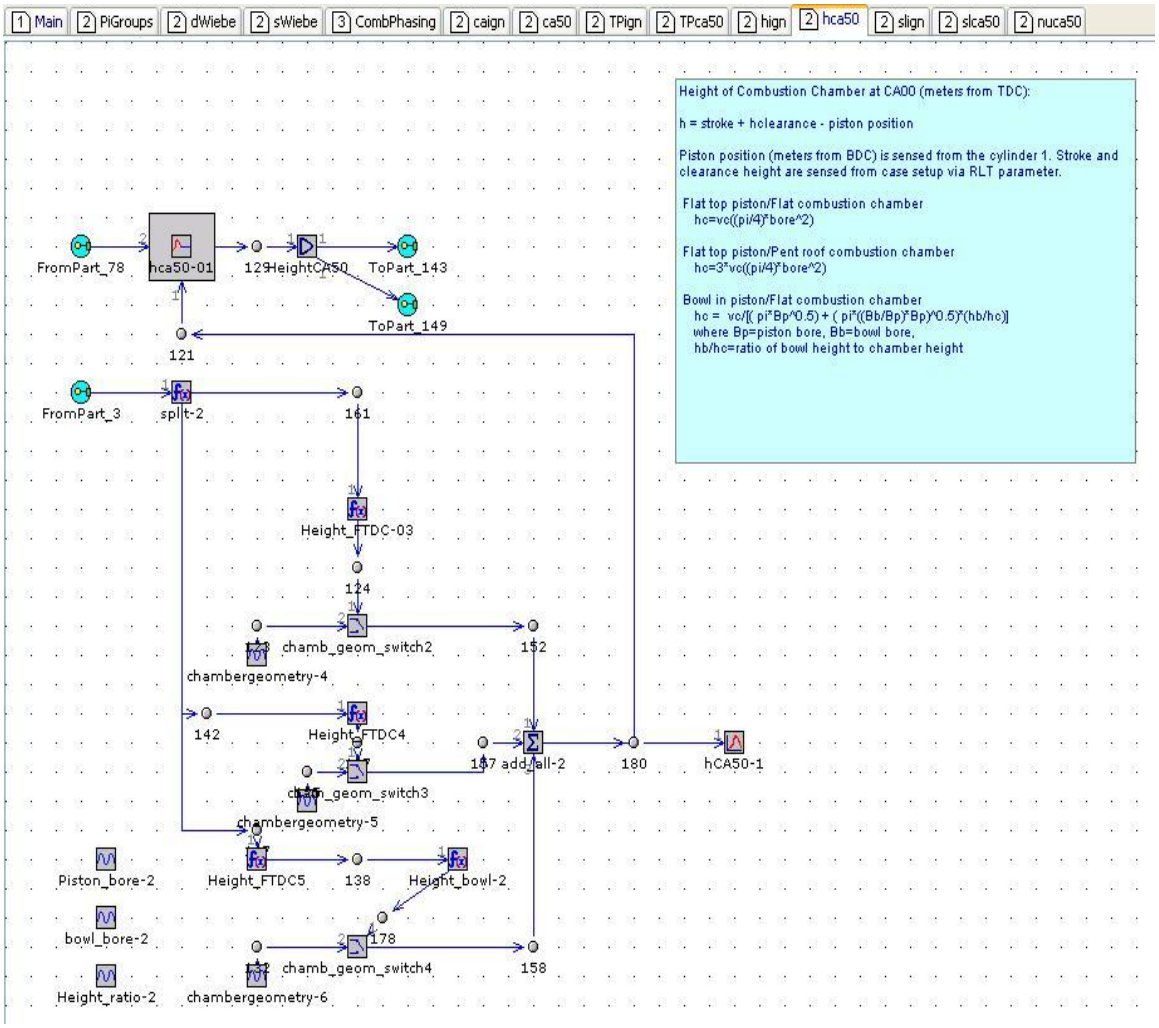

Updated clearance height calculations at ignition point (h_{CA50})